NASA TECHNICAL NOTE

NASA TN D-7874 c.1

4D AREA NAVIGATION SYSTEM DESCRIPTION AND FLIGHT TEST RESULTS

Homer Q. Lee, Frank Neuman, and Gordon H. Hardy

Ames Research Center
Moffett Field, Calif. 94035

NATIONAL AERONAUTICS AND SPACE ADMINISTRATION • WASHINGTON, D. C. • AUGUST 1975

1. Report No.	2. Government Accession No.	3. Recipient's Catalog No.
TN D-7874		

4. Title and Subtitle	5. Report Date
4D AREA NAVIGATION SYSTEM DESCRIPTION AND FLIGHT TEST RESULTS	August 1975
	6. Performing Organization Code

7. Author(s)	8. Performing Organization Report No.
Homer Q. Lee, Frank Neuman, and Gordon H. Hardy	A-5788
	10. Work Unit No.
9. Performing Organization Name and Address	501-03-11
Ames Research Center Moffett Field, Calif. 94035	11. Contract or Grant No.
	13. Type of Report and Period Covered
12. Sponsoring Agency Name and Address	Technical Note
National Aeronautics and Space Administration Washington, D.C. 20546	14. Sponsoring Agency Code

15. Supplementary Notes

16. Abstract

A 4D area navigation system was designed to guide aircraft along a prespecified flight path (reference path) such that the aircraft would arrive at the approach gate at a time specified by the ATC controller. Key components to achieve this requirement were: (1) stored reference trajectories; (2) a continuously recomputed capture trajectory to a selected waypoint on the reference trajectory so as to achieve the desired time of arrival; (3) electronic situation displays; and (4) a control system to follow the overall trajectory in space and time.

The system was implemented in a digital integrated avionics system (STOLAND) installed on a CV-340 airplane. Although the 4D system was designed primarily for automatic operation, it was flight tested in a flight director mode (the pilot follows the flight director commands), because the CV-340 autopilot servos were not tied to the avionics system. The flight test showed that, even in the flight director mode, the pilot did achieve the objectives of path tracking and time of arrival control with only moderate workload. The system also permitted controlled delay of the time of arrival by path stretching, which takes advantage of the continuously changing capture trajectory to predict the time of arrival. While time of arrival was controlled to within less than 5 sec, more work is needed to minimize throttle activity in the presence of varying winds and navigation errors.

Simulations in the automatic and manual modes were used to complement the flight data.

17. Key Words (Suggested by Author(s))	18. Distribution Statement
Air navigation system Air traffic control	Unclassified - Unlimited STAR Category - 04

19. Security Classif. (of this report)	20. Security Classif. (of this page)	21. No. of Pages	22. Price*
Unclassified	Unclassified	61	$4.25

*For sale by the National Technical Information Service, Springfield, Virginia 22161

TABLE OF CONTENTS

SYMBOLS

A	specified ground acceleration
D_k	horizontal distance subtended by straight flight for waypoint k
$DELD_K$	horizontal distance subtended by a turn for waypoint k
DIST(t)	horizontal distance traversed by the phantom aircraft since the beginning of a command segment
EWANGL, EWMAG	keyboard entry of estimated angle and magnitude of wind
g	acceleration of gravity
$ENTRIM_K$	nominal time required to fly the aircraft from waypoint k to the approach gate
H(t)	ground-track heading
H_a	ground-track heading of the aircraft
H_i	reference ground-track heading at the beginning of the ith command segment
H_{k+1}	ground-track heading computed for waypoint k
k_{vx}, k_{vy}, $k_{\phi x}$, $k_{\phi y}$, $k_{\phi\psi}$, k_{zz}	gains for x, y, ψ, and z feedbacks
NWP	total number of waypoints
R_i	turning radius for the ith command segment
R_k	turning radius specified for waypoint k
$TMAX_K$	maximum time required to fly from waypoint k to the approach gate
$TMIN_K$	minimum time required to fly from waypoint k to the approach gate
$TSHIFA_K$	time available for advancing (earlier arrival) TOA at waypoint k
$TSHIFD_K$	time available for delaying (later arrival) TOA at waypoint k
VA_k	airspeed specified for waypoint k

VDIST	horizontal distance subtended while decelerating from speed VQ_{k-1} to VP_k
$V_c(t)$	command airspeed for automatic tracking
$V_c'(t)$	command airspeed for manual tracking
$V_i(t)$	reference ground speed
V_{io}	reference ground speed at the beginning of the ith command segment
$\dot{V}_i$	acceleration command for the ith command segment
Vr(t)	reference airspeed
VP_k	ground speed at the beginning of a turn for waypoint k
VQ_k	ground speed at the end of a turn for waypoint k
$V_a(t)$	aircraft speed in IAS
$V_x(t)$, $V_y(t)$, $V_z(t)$	x, y, z components of the reference airspeed V_r*
x(t), y(t), z(t)	deviation of actual aircraft from the phantom in moving target reference coordinates
$X_a(t)$, $Y_a(t)$, $Z_a(t)$	position coordinates of the aircraft*
$X_r(t)$, $Y_r(t)$, $Z_r(t)$	reference position coordinates*
X_{ro}, Y_{ro}, Z_{ro}	reference position coordinates at the beginning of a command segment*
X_c, Y_c	coordinates of a center of a turn*
$\dot{X}(t)$, $\dot{Y}(t)$, $\dot{Z}(t)$	component of the reference ground speed $V_a(t)$*
W_{xe}, W_{ye}, W_{ze}	components of the wind speed as estimated by the navigation filter*

*In runway coordinates

$\gamma_c(t)$	commanded flight-path angle (for automatic tracking)
$\gamma_c'(t)$	commanded flight-path angle (for manual tracking)
γ_i'	flight-path angle for the ith commanded segment
γ_k	flight-path angle computed for waypoint k
γ_{max}, γ_{min}	maximum and minimum allowable flight-path angles
$\dot{\gamma}_{max}$	maximum allowable flight-path angle rate
ΔT_i	time duration for flying at constant speed VQ_{k-1} in a nominal TOA trajectory
ΔT_{i+1}	time duration for decelerating from speed VQ_{k-1} to VP_k
ΔT_{i+2}	time duration for flying at constant speed VP_k in a nominal TOA trajectory
ΔT_{i+3}	time duration for decelerating from speed VP_k to VQ_{k-1}
ΔT_P	time duration for flying at constant speed VP_k in a maximum time of arrival trajectory
ΔT_Q	time duration for flying at constant speed VQ_{k-1} in a minimum time of arrival trajectory
$\Delta V(Z_a)$	correction factor for changing from TAS to IAS ($\Delta V(Z_a)$ is a function of aircraft altitude)
ρ	index for adjusting TOA by speed control alone, $\rho \varepsilon [0,1]$
τ_γ	lead time for flight-path angle command
τ_ϕ	lead time for bank angle command
$\phi_a(t)$	bank angle of the aircraft
$\phi_c(t)$	bank angle command (for automatic tracking)
$\phi_c'(t)$	bank angle command (for manual tracking)
$\phi_r(t)$	reference bank angle
$\phi_{r,i}$	the reference bank angle at the end of the ith command segment
$\phi_{r,i+1}$	the reference bank angle at the beginning of the i+1 command segment
ϕ_{max}	maximum allowable bank angle

$\dot{\phi}_{max}$	maximum allowable bank angle rate
$\psi(t)$	heading error
$\Psi_a(t)$	aircraft heading
$\Psi_r(t)$	reference aircraft heading
$\dot{\phi}_a(t)$	roll rate of aircraft
$\dot{\theta}_a(t)$	pitch rate of aircraft
x, y, z	components for deviation of actual aircraft from the phantom, in moving target reference coordinates
X_a, Y_a, Z_a	position coordinates of aircraft*
X_r, Y_r, Z_r	reference position coordinates*
XWP_k, YWP_k, ZWP_k	position coordinates specified for waypoint k

Subscripts

i	ith command segment
k	waypoint k
r	reference quantities
a	aircraft quantities
nf	navigation filter
kb	keyboard entry

*In runway coordinates

ACRONYMS

ATC	air traffic control
EADI	electronic altitude display indicator (see fig. 5)
MODILS	modular instrument landing system
MFD	multifunction display (see fig. 4)
MLS	microwave landing system
RNAV	area navigation
STOLAND	a digital integrated avionics system primary for STOL aircraft
SAS	stability augmentation system
TACAN	tactical air navigation
TOA	time of arrival
WPT	waypoint

Mnemonics for Keyboard Entry

FOD	= 1, flight conventional mode
	$\neq$ 1, flight Ames 4D mode
EWD	wind entry, as input to Ames 4D
SWD	wind estimated, monitoring
TDC	time delay change

Abbreviations for On-Off Buttons in Control Panel

FP1, FP2, FP3, FP4	flight paths 1, 2, 3, 4, respectively
REF F.P.	engaging the system in flight director mode (reference flight path)
FULL AUTO	engaging the system in automatic mode (fully automatic)
F/D	flight director

Abbreviations for MFD Display

TWP	predicted time of arrival at the waypoint specified, sec
ALT	altitude of next waypoint, ft

TOA	time of arrival, hr:min:sec
TDA	time available for delaying and advancing TOA
NOCAP HOR	no horizontal flight path for capturing the next specified waypoint exists
NOCAP ALT	no vertical profile (for capturing the specified waypoint) exists
NOCAP VEL	no speed profile (for capturing the specified waypoint) exists
CALT	capture altitude, ft
ERROR ALT	altitude error exceeded the prespecified value
ERROR Y	cross track error exceeded the prespecified value
ERROR X	along track error exceeded the prespecified value
FLP 17	17° flap
FLP 28	28° flap
FLP 40	40° flap

4D AREA NAVIGATION SYSTEM DESCRIPTION

AND FLIGHT TEST RESULTS

Homer Q. Lee, Frank Neuman, and Gordon H. Hardy
Ames Research Center

SUMMARY

A 4D area navigation system was designed to guide aircraft along a prespecified flight path (reference path) such that the aircraft would arrive at the approach gate at a time specified by the ATC controller. Key components to achieve this requirement were: (1) stored reference trajectories; (2) a continuously recomputed capture trajectory to a selected waypoint on the reference trajectory so as to achieve the desired time of arrival; (3) electronic situation displays; and (4) a control system to follow the overall trajectory in space and time.

The system was implemented in a digital integrated avionics system (STOLAND) installed on a CV-340 airplane. Although the 4D system was designed primarily for automatic operation, it was flight tested in a flight director mode (the pilot follows the flight director commands), because the CV-340 autopilot servos were not tied to the avionics system. The flight test showed that, even in the flight director mode, the pilot did achieve the objectives of path tracking and time of arrival control with only moderate workload. The system also permitted controlled delay of the time of arrival by path stretching, which takes advantage of the continuously changing capture trajectory to predict the time of arrival. While time of arrival was controlled to within less than 5 sec, more work is needed to minimize throttle activity in the presence of varying winds and navigation errors.

Simulations in the automatic and manual modes were used to complement the flight data.

INTRODUCTION

Guidance and navigation systems for short-haul aircraft of the future will need to meet stringent requirements to fully utilize the capability of STOL aircraft to fly tight turns, at low speeds, and at steeper descent angles than CTOL aircraft. Analytical and simulation studies (refs. 1 to 4) have resulted in a 4D guidance concept that can provide the precision of flight path and time control which may be required for STOL aircraft. These investigations were based on requirements outlined in references 5 and 6.

The system was flight tested to provide information on the system-to-pilot interface, pilot acceptance, and effects of the imperfect knowledge of the navigation and wind data on guidance and control performance. Flight test results will provide a basis for further system design improvements. A versatile digital avionics research system called STOLAND (ref. 7) was available in a CV-340 aircraft to implement the essential portions of the 4D guidance system. Although the CV-340 is a CTOL aircraft, typical STOL approaches were flown. The STOLAND system was designed for test purposes. First, the system is equipped with a precise terminal area navigation system (ref. 8). Second, it includes another type of 4D guidance system (ref. 9), which provided many pilot-to-system interfaces in the form of computer programs and hardware that are required for the system under study.

The system tests reported in reference 9 concerned the precision of tracking a fixed reference flight path under actual environmental conditions; due to system limitations, the time of arrival at the approach gate was not known before the acquisition of the first selected waypoint. The primary goal of the current study was to determine the pilot-systems interaction under simulated changes in air traffic control conditions. This report presents the flight experience of a 4D system that computes time of arrival at the approach gate continuously from any aircraft position via a combination of a capture trajectory, which originates at the aircraft, and a fixed reference flight path.

Simulation experiment results, complementing those from the flight test, are also reported. The simulation experiments permit fully automatic operation of the system with all displays and input devices operating in the simulator cab. Flight experiments were conducted in the flight director mode only, since the autopilot servos were not tied to the system in the CV-340 test aircraft.

TECHNICAL SUMMARY OF THE AMES 4D RNAV SYSTEM

The 4D RNAV system was designed to provide precise spacing of STOL aircraft arrivals and accurate execution of air traffic controller (ATC) instructions. It will minimize delays and interference with CTOL traffic by reducing the amount of airspace used by the aircraft.

The tests assume that when the aircraft enters the airspace controlled by the terminal area ATC, it will be assigned a specific STOL approach route (reference flight path) and a required time of arrival (TOA) at waypoint 6 (sketch (a)). To predict the TOA, aircraft position and velocity must be known accurately, and a complete flight path from its present position to waypoint 6 must be defined. In general, the aircraft will not be on the specified STOL approach route initially, and the complete flight path will not be known. One solution is to generate in the airplane a flight path called a capture flight path, which connects the present aircraft position with a selected waypoint on the assigned STOL approach route. The capture flight path together with the STOL approach route form a complete flight path, which is neeeded for time-controlled guidance.

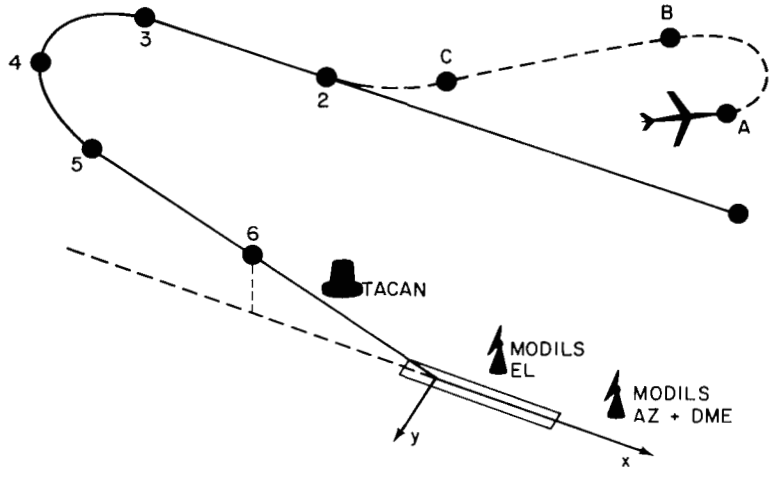

Sketch (a)

The navigation portion of the system (ref. 8) provides an estimate of the aircraft position and velocity. The external navigation signals are TACAN for large area coverage, and the scanning beam MLS (MODILS) for high precision during final approach and landing. In addition, aircraft attitude, linear accelerations, barometric altitude, and airspeed are used with complementary filters to obtain the aircraft position and velocity. A wind vector is estimated from the difference between inertial and air data.

The guidance system is based on generating the capture flight path and on controlling both time and position along the capture flight path and the fixed STOL approach route, both of which are defined by waypoints. Waypoint coordinates are stored in the onboard computer along with such information as the radius of turn, and the maximum, minimum, and nominal airspeeds at waypoints.

The generation and definition of the capture flight path will now be discussed. The capture flight path connects the present aircraft position with waypoint 2 (or any waypoint selected by the pilot) on the STOL approach route. The capture path consists of a turn, a straight segment, and another turn. It is defined by waypoints A to C, where A is specified by the initial position, altitude, heading, and speed of the aircraft. While the aircraft maneuvers in the terminal area, a new capture flight path and the time of arrival at waypoint 6, which is the final waypoint for the 4D RNAV, are continuously recomputed and displayed to the pilot.

The system has two modes, the predictive mode and the track mode. In the predictive mode, the pilot selects the waypoint of the reference flight path to be captured. He inputs a wind estimate for the path, which is used for the speed profile calculations. (Since wind tends to decrease with lower altitude this procedure is believed preferable to using the navigation system's present estimate of the wind.) To achieve the ATC specified arrival time at waypoint 6, the pilot maneuvers the aircraft until the predicted and required TOA on the display agree. He then commands the system to fix the capture flight path and begin tracking.

In the track mode, the pilot flies the reference flight path using the flight director for guidance. (In the simulation, automatic tracking was possible; in the flight test, only flight director guidance was available.) Slightly before waypoint 3 on the approach path, a predictive bank angle command is given, and just before waypoint 4, a constant vertical acceleration maneuver is performed to acquire the 5° flight-path angle used in this investigation. The short straight-in-section (waypoints 5 and 6) is the last segment using the 4D guidance laws. The remaining flight path to flare is flown with lateral and vertical guidance laws, similar to those used for 4D RNAV except that they have higher system gains to assure precise path tracking.

The principal constituents of the onboard computer program are the flight path synthesizer and the control law. The flight path synthesizer generates either onboard or on the ground, command tables for approach paths from a minimum set of information, so that aircraft constraints are not violated. A command table consists of a series of autopilot or flight director commands and their corresponding time duration. The command table for the example in sketch (a) is shown in sketch (b). The aircraft descends at the appropriate flight

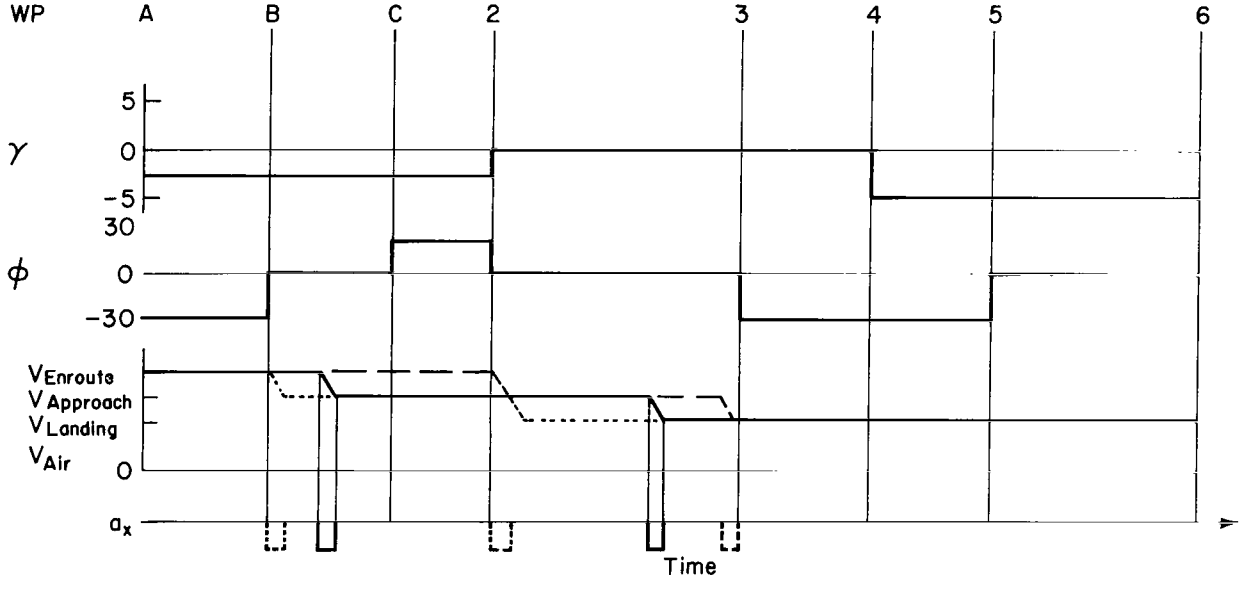

Sketch (b)

path angle to intercept waypoint 2, flies level until waypoint 4, and then begins a 5° turning descent. Similarly, the nominal roll angles are shown to execute the turns from A-B, C-2, and 3-5. Note that the table is computed under the assumption of infinite flight-path angle and bank angle rates. The control system compensates for these simplifying assumptions.

An acceleration schedule also is calculated which, together with the wind information and aircraft speed constraints (discussed later), permits TOA calculations. In this system, it is required that deceleration takes place between adjacent waypoints. The initial placement of the decelerating segments is such that it is possible to change the time of arrival by the same amount in both directions. By changing the deceleration to begin at waypoints B and 2 (dotted line) or to terminate the deceleration at C and 3 (dashed line) the maximum change in possible TOAs is calculated and displayed to the pilot.

From the command sequence table generated by the guidance calculations and the reference flight path coordinates, the control law continuously generates reference states of the aircraft's position and speed. The horizontal reference position, also called phantom position, and the actual aircraft position are displayed to the pilot. The control law compared the reference and the actual aircraft states and generates commands for pitch, roll and speed. In addition, the control law generates commands for pitch and roll maneuvers somewhat ahead of the reference values to compensate for the simplifying assumptions of infinite rates made in the guidance computations. These commands are applied to the longitudinal and lateral control system and autothrottle in the automatic control mode, and to the electronic altitude display indicator (EADI) flight director bars and speed error indicator in the manual control mode. When needed, based on speed, flap deployment messages and guidance error messages are generated to help the pilot in his task. For safety, the speed command is limited from above by the flap placard structural limit and from below by a margin above the stall speed, which is computed from the aircraft bank angle and configuration. These aircraft speed constraints are also used for time of arrival calculations.

The synthesized reference flight path that was flown in the flight test is shown in figure 1. It consisted of six waypoints, each is specified by the X, Y, Z coordinates in km and the desired indicated airspeed in knots.

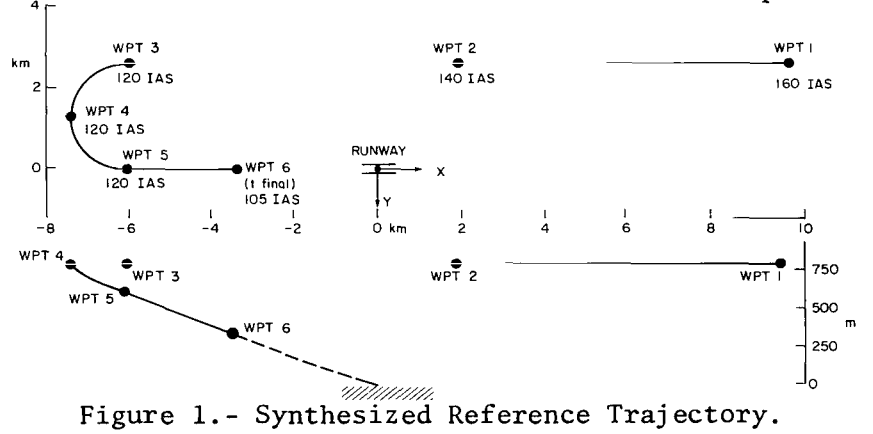

Figure 1.- Synthesized Reference Trajectory.

The technical details of the system that are not reported in references 1 to 4 are described in appendix A.

PILOT'S OPERATING PROCEDURE

Displays and Input Devices

The major input devices to the system are the mode select panel (MSP) and the keyboard (figs. 2 and 3). The MSP enables the pilot to engage conventional autopilot modes (e.g., to select and hold heading, speed and altitudes) and to switch from a predictive 4D RNAV mode to the capture and track modes. The keyboard allows the pilot to engage the 4D in a predictive mode to input wind estimates, to advance or delay TOA, and to specify the waypoint to be captured.

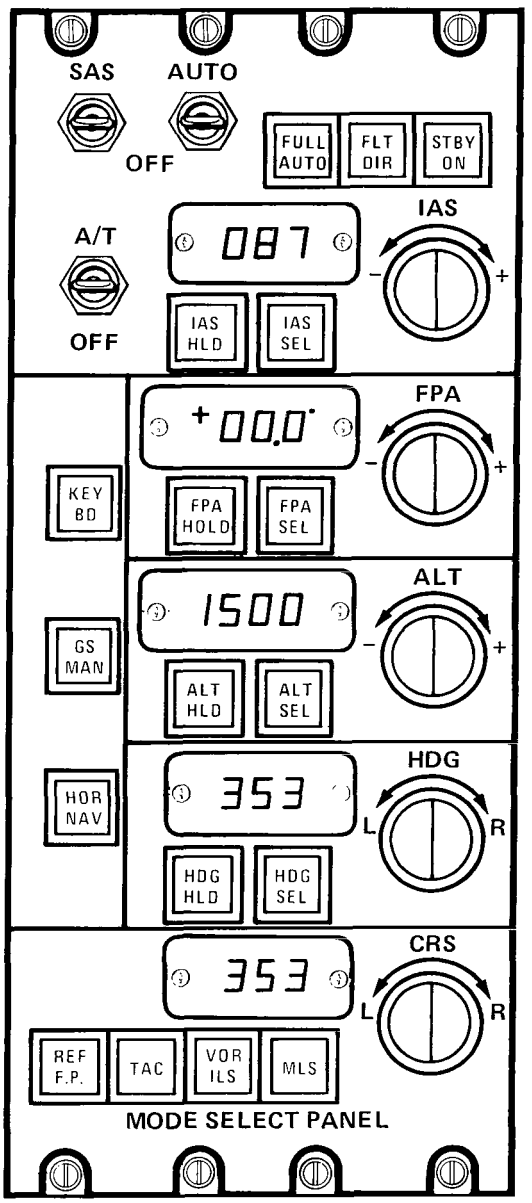

Figure 2.- Mode Select Panel (MSP).

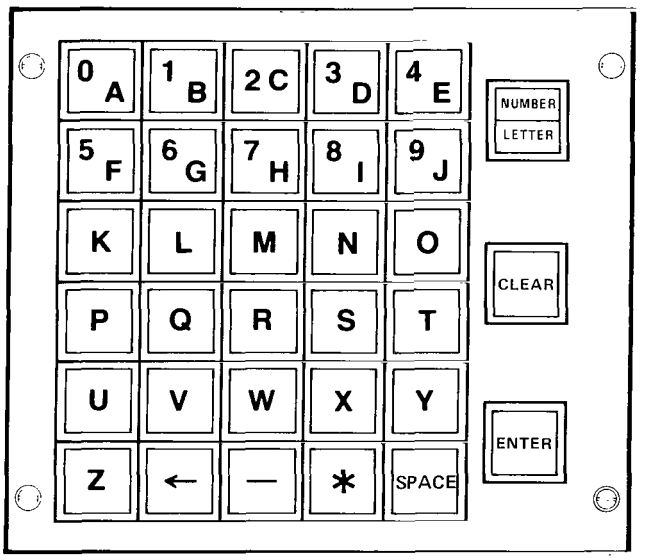

Figure 3.- Keyboard.

The major output devices are multifunction display (MFD, fig. 4), the electronic attitude director indicator (EADI, fig. 5), and the status panel (fig. 6). The MFD displays the reference flight path, the capture trajectory, the position and heading of both the phantom (reference position) and the actual aircraft, the current clock-time (on the upper right corner), the barometric altitude in feet (on the upper left corner)

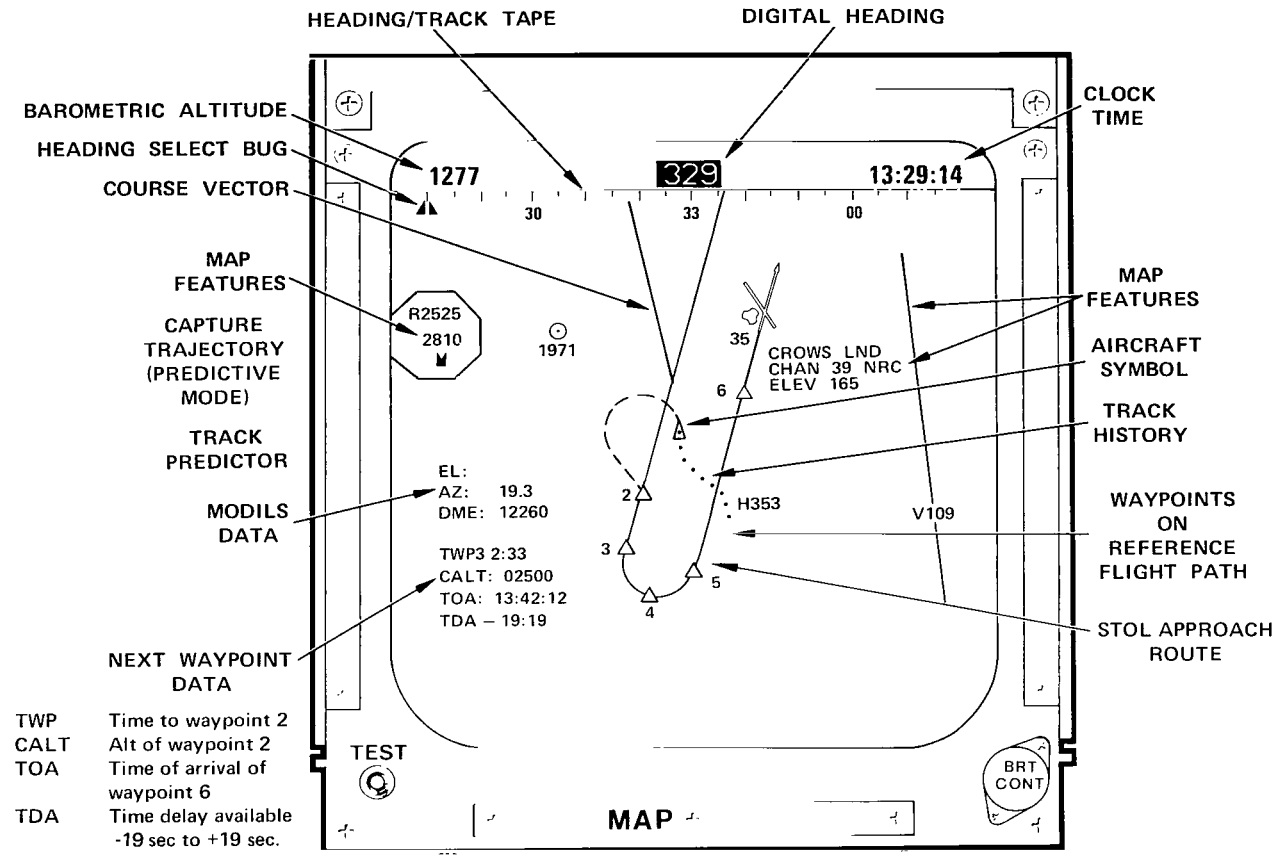

(a) Predictive mode (north up).

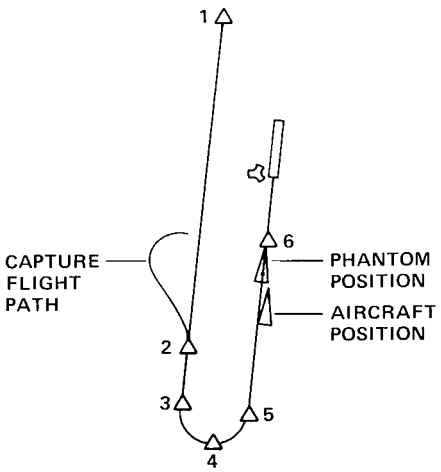

(b) Track mode.

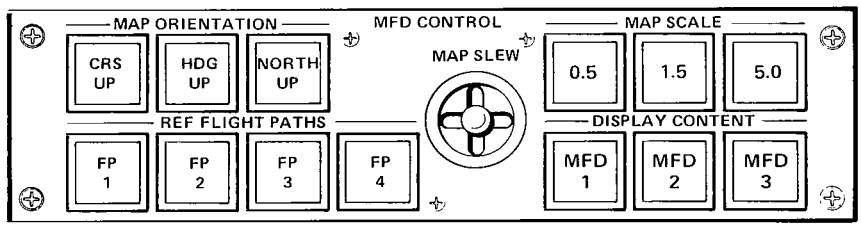

(c) Control panel.

Figure 4.- MFD display.

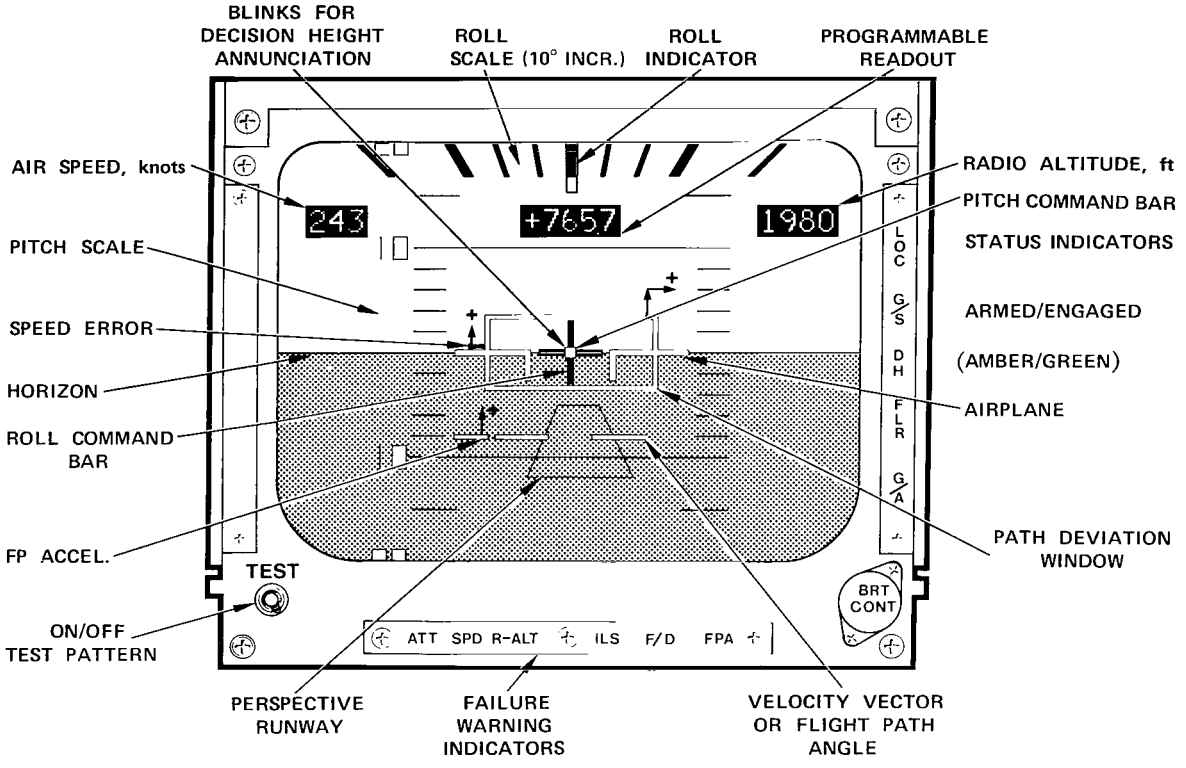

Figure 5.- Electronic attitude director indicator.

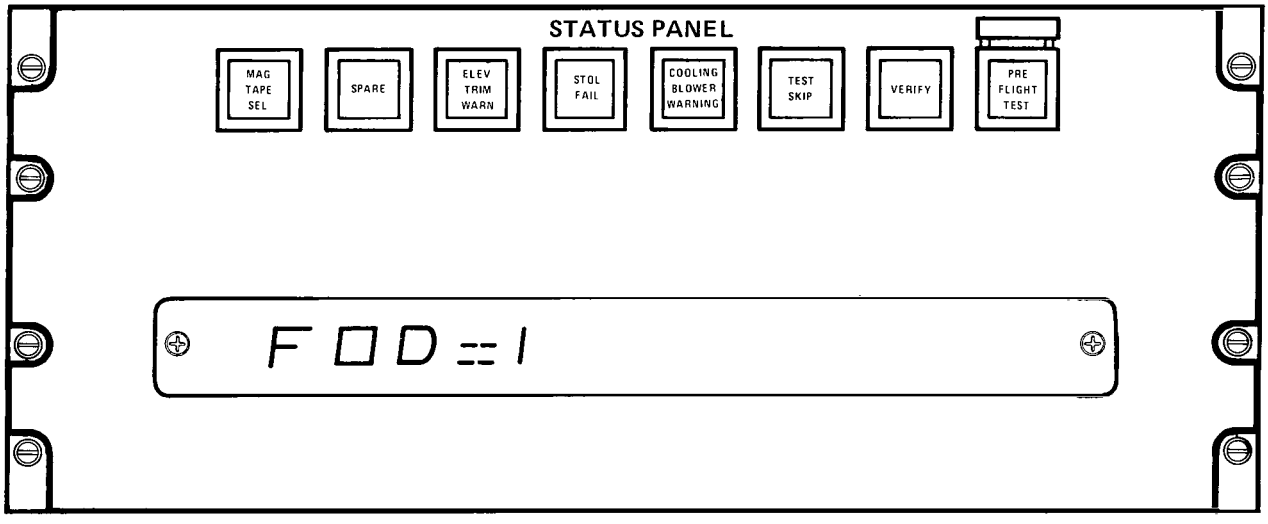

Figure 6.- Status panel.

and other alphanumeric messages. The phantom (fig. 4(b)) is the reference or desired position, where the aircraft should be if the control system errors are nulled. The EADI displays the flight director bars: the speed error bar, the pitch command bar and the roll command bar. These bars are used by the pilot to fly the flight director mode. The status panel informs the pilot of failure conditions and validity of keyboard inputs.

RNAV Modes

The 4D RNAV system operates in two distinct modes, the predictive mode and the track mode. In the predictive mode, the pilot is free to fly the airplane as he wishes using the conventional autopilot or flight director modes if desired. The system merely calculates a capture flight path from the present airplane position to a selected waypoint on the approach flight path, and it predicts the arrival time at the final waypoint if the pilot were to engage the system at this instant. Once the pilot engages the system to achieve a desired arrival time, the system disengages the conventional modes and switches to the 4D track mode. In that mode, the system tracks the last computed capture flight path onto the stored STOL approach route and then tracks it in such a manner that it will arrive at the final waypoint at the predicted time, while observing various operational limits.

Operating procedure in the predictive mode- The operating procedure in this mode is summarized below. To synthesize an overall flight profile, the pilot must:

1. Enable Ames 4D by entering FOD=1 on the keyboard.

2. Select a stored STOL approach route such as FP2 on the MFD control panel.

3. Select navaid by pressing TACAN, for example, on MSP.

4. Specify waypoint to be captured (target waypoint) by a keyboard entry, for example, WPT = 5.

5. Input wind estimate by keyboard entry.

To get the system ready for track, the pilot must maneuver the aircraft so TOA is as desired.

The system responds to (1) through (4) by synthesizing a capture flight path from the current aircraft position to the target waypoint. It responds to (5) by synthesizing a new ground speed profile including one for the capture flight path, and generating a new table of commands.

The operating procedure in the predictive mode will be illustrated by an example. In order to synthesize an overall flight profile, 4D must be engaged by entering FOD=1 on the keyboard. (When FOD=0, a different 4D system is available to the pilot, which has been described in ref. 9.) At this stage, the pilot has the option of selecting one of the four available reference flight paths by depressing one of the four buttons, FP1, FP2, FP3, and FP4 in the MFD control panel. This will cause the selected reference flight path to be displayed on the MFD. The current aircraft position is transmitted to the 4D RNAV system after some navaid has been selected, for example, by depressing TACAN button in the MSP. After navaid selection, a bright steady isosceles triangle, indicating the position and heading of the aircraft will appear on the MFD to signify that the position estimate calculation has reached its

steady state. (A flashing triangle indicates the navigation computations are still in the converging process.) The desired waypoint to be captured on the STOL approach route is specified by inputting WPT=n on the keyboard, where n is the desired waypoint (e.g., WPT 5). The waypoint number must be one of the waypoints displayed on the reference flight path.

If not, an ILLEGAL ENTRY will be displayed on the status panel. If a capture trajectory exists, it will be displayed on the MFD as a dotted line, and the standard four-line message, having the following format displayed:

TWP 5 1:51
ALT 3500
TOA 1:45:30
TDA-19:19

In the first line, the message means that the next waypoint (capture waypoint) is waypoint 5 and the flying time to waypoint 5 is 1 min and 51 sec. The second line displays the altitude for waypoint 5 (3500 feet or 1068 m). The third line displays the predicted time of arrival at the final waypoint, 1 o'clock, 45 min and 30 sec. And the fourth line states the time available for advancing TOA (for an earlier arrival) is -19 sec and for delaying TOA is also 19 sec. The adjustment of TOA is computed on the basis of providing the pilot with equal flexibility in advancing or delaying TOA after the system is placed in track. If a capture trajectory cannot be synthesized, then a two-line message is displayed: a flashing first line and a steady second line having the following formats:

NOCAP HOR 5 or NOCAP ALT 5 or NOCAP VEL 5

CALT 3500

where 5 is the target waypoint number and 3500 ft (1068 m) is the altitude of the waypoint. NOCAP HOR 5 means no horizontal capture trajectory exists and none is drawn on the MFD. NOCAP ALT 5 means the difference between the current and target altitudes divided by the horizontal path length (synthesized for the horizontal capture trajectory) is beyond the range of the allowable flight path angle. Finally, NOCAP VEL 5 means it is not possible to decelerate (or accelerate) from the current airspeed to that specified for waypoint 5 and therefore no speed profile.

The wind input is entered at the keyboard by inputting the mnemonic EWD 123°.20, where 123 is the wind direction (in deg) with respect to magnetic North and 20 is the wind speed (in knots). To aid the pilot in selecting a reasonable wind estimate in flight, the numerical values of wind angle and wind magnitude, as estimated by the navigation filter, can be obtained by entering at the keyboard the mnemonic SWD. The range of wind direction is restricted to (0, 359) and for the wind magnitude to (0,999). Should a value outside either of these ranges be entered, an ILLEGAL ENTRY message will be displayed on the status panel. Otherwise, the keyboard input will be processed, and the new values of TOA and TDC will be computed and displayed on the MFD.

The next step is to fly the aircraft until the displayed TOA is as desired. In doing so, the pilot should fly the aircraft in such a way that the capture trajectory always exists. This can always be done by maintaining an altitude and speed fairly close to those specified at the waypoint to be captured, and by maintaining a reasonable distance and heading with respect to those of the waypoint to be captured. It will remain practically constant if the aircraft is flying along the capture trajectory, since the capture trajectory gets shorter as time passes (sketch c (a)). It will increase about the same rate as real time when the aircraft is flying perpendicular to the reference flight path, since the length of the capture flight path changes little as time passes (sketch c (b)). TOA increases at about twice the rate as real time if flying in the opposite direction to the reference flight path, since the capture flight path gets longer as time passes (sketch c (c)). The TOA also can be adjusted for an earlier arrival by capturing a higher numbered waypoint (sketch C (d)).

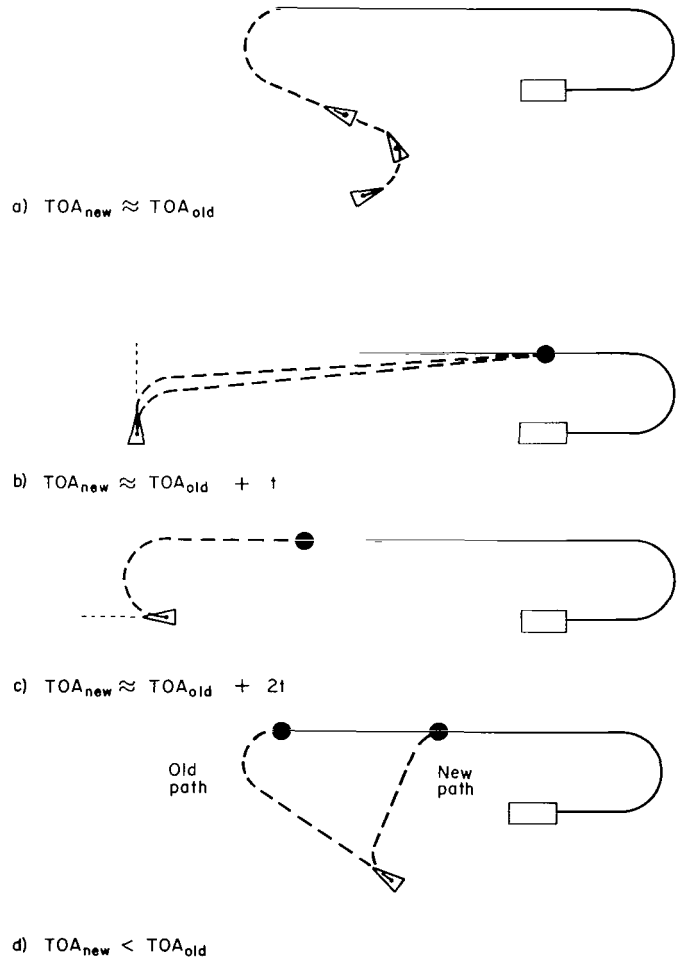

Sketch (c)

Operating procedure in track mode- When the desired TOA is reached, the system should be placed in track immediately. This is done by depressing the REF F.P. button on the MSP for manual tracking and the FULL AUTO button for automatic tracking. In manual tracking, the F/D button must also be on so that the speed, pitch, and roll command bars will be displayed on the EADI.

After the system is in track, the appropriate REF F.P. or FULL AUTO light will turn green. If for some reason the system is not ready for track after one of these buttons is pushed — that is, no capture trajectory exists — then the REFP (or FULL AUTO) light will turn amber and the system will continue to synthesize a capture trajectory. At the moment the system is ready for track, the REF FP (or FULL AUTO) light will turn green and the system will place itself in track automatically.

In the track mode, TOA is frozen and the capture trajectory is displayed as a solid line. Furthermore, a dim isosceles triangle, indicating the position and heading of the phantom aircraft (as contrasted to the bright isosceles triangle for the aircraft) will appear on the MFD.

Once the system is in track, it will remain in track until it is interrupted by either pilot inputs or until it automatically switches to a conventional glide slope and localizer track mode at the final waypoint. The pilot can take the system out of track and thus disengaging REF FP or FULL AUTO by pressing the appropriate button on the MSP or by inputting a different wind on the keyboard. In track, the time of arrival may now be adjusted to achieve the desired TOA, which may differ from the TOA on display by a few seconds. The adjustment is made by exercising the TDC input.

The time delay input is entered at the keyboard by pressing TDC mm.ss or TDC - mm.ss, where mm and ss are shifts in TOA in minutes and seconds, respectively, with a negative sign for advancing TOA (or earlier arrival). The value of TDC input must be within the range of TDA as displayed in the fourth line on the MFD. If so, the input is processed and is reflected on the value of both TOA and TDC lines. Otherwise an ILLEGAL ENTRY message will be displayed on the status panel and the input is ignored.

A time delay outside the range can be achieved by a path-stretching maneuver. Essentially, the pilot first switches the system back to predictive mode by depressing the REF FP or FULL AUTO button and flies away from the reference trajectory until the desired TOA is displayed. At that time, he reengages the system. While the system is in the predictive mode, a time change could also be achieved by capturing a different waypoint.

If it should be desirable to enter a wind estimate from the keyboard while the system is in track, the system will process the wind entry and automatically switch back to the predictive mode. Next, it will proceed to synthesize a capture trajectory to the next waypoint and if one exists, it will display it as a dotted line on the MFD system. If the pilot presses REF FP (or FULL AUTO) button again, this path will be followed.

After the system is again in track, the pilot should observe the change in TOA and may make fine adjustments to keep the old TOA by exercising the TDC command, if desired.

Displays for pilot convenience in the track mode- The excessive error message and the flap-deployment message will be on display under certain prescribed conditions. A flashing message ERROR ALT or ERROR Y or ERROR X will be displayed on the MFD should the altitude, cross-track, or along-track errors exceed some value stored in the digital computer. If more than one excessive error occur simultaneously, then the message will display the error highest in the display hierarchy, which is of the following descending order: altitude error, cross-track error, and along-track error. The cross-track and along-track error can be observed from the deviation of the aircraft position from that of the phantom. The cross-track and altitude errors also are displayed on the EADI. A lateral displacement of the rectangular box on the EADI from the center reflects the cross-track error and a vertical displacement reflects altitude error.

The second message is the flap-deployment message, which reminds the pilot when to deploy the flap manually to provide adequate stall margins. In the CV-340, the flap-deployment messages are based on the IAS and bank angle of the aircraft. The message FLP 17, FLP 28, or FLP 40 will be displayed at the proper airspeeds. However, no flap message is displayed while flying the capture flight path, and the 40° flap message is displayed only at the final glide slope.

Pilot procedure for large guidance error- The pilot is cautioned that the control system is designed on a linear perturbation control law. If the aircraft deviates too far from the phantom, then the command may be meaningless. In this case, the pilot may reduce the error by observing raw errors or simply by reinitializing the phantom (by pressing REF FP twice, the first time for disengaging the system so that a new capture trajectory is synthesized, and the second time for placing the system in track). The reinitialization process automatically reduces all errors to zero. After the system is again in track it may be necessary to exercise the TDC command to maintain the same TOA. Should a flashing NOCAP N be displayed, where N is the number of the selected waypoint after the system is out of track, then the pilot must maneuver the airplane until a new capture flight path is synthesized before he can press the REF FP button to reinitiate track.

FLIGHT AND SIMULATION EXPERIMENT RESULTS

Flight Test Procedure and Facilities

The STOL test facility (fig. 7) includes an experimental scanning beam microwave landing system MODILS (modular Instrument Landing System, ref. 8) and a local TACAN station for which the terminal area navigation system was

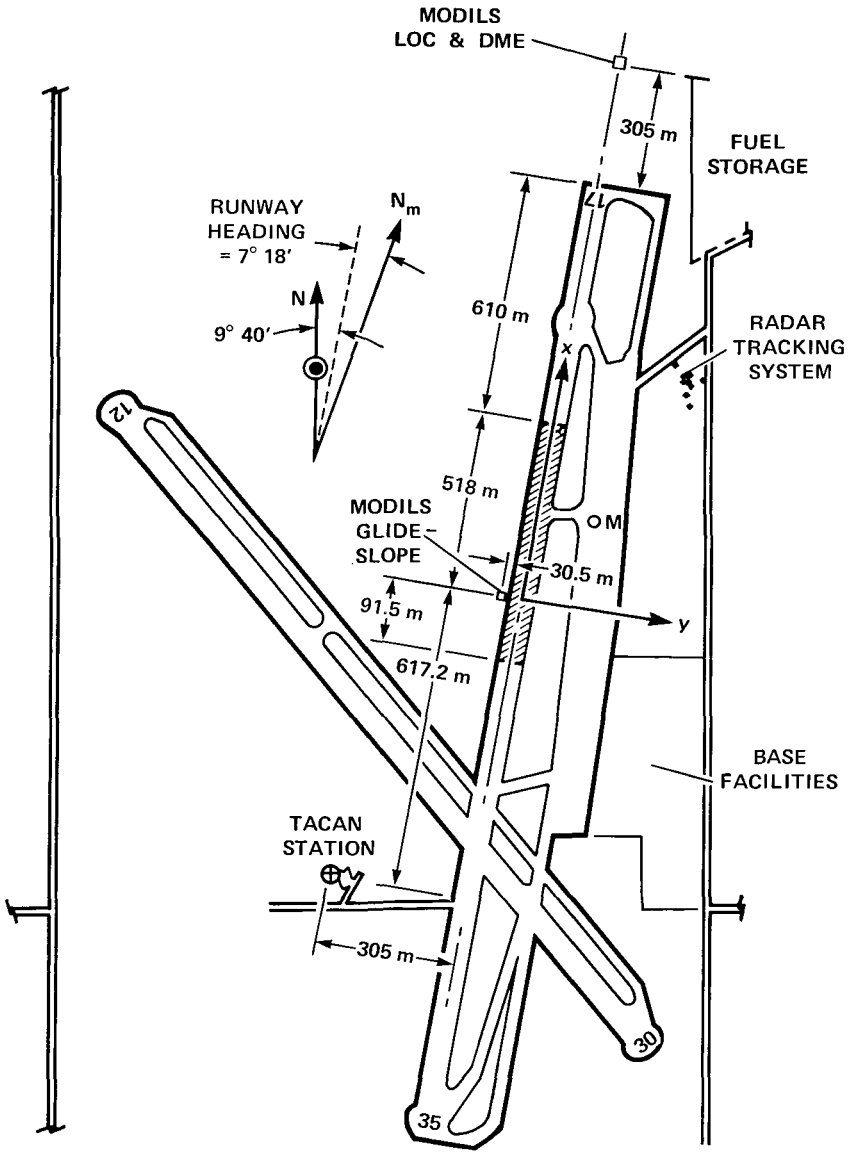

Figure 7.- NASA STOL test facility at Crows Landing Naval Air Station, Calif.

specifically designed (ref. 8). The STOL approach route descirbed earlier is oriented with respect to the navigation coordinate system, the origin of which is at the center of the runway and the intersection of the perpendicular from the position of the MODILS glide slope antenna to the runway centerline.

For the test, the pilot was aided by the flight test conductor, who had two functions: First, he simulated ground-to-aircraft ATC commands (e.g., "arrive at the approach gate at TOA 13:42:12," which is a specific time). Second, he also participated actively in the test, because some system elements as installed in the CV-340, were inaccessible to the pilot. At the pilot's command, he entered keyboard messages the pilot called out and read messages from the status panel to the pilot.

Two hours of flight time were devoted to the Ames 4D phase of the system flight tests. This flight time together with extensive simulator experiments, was sufficient to evaluate the performance of the Ames 4D system.

Quantitative Results

Flight test overview- The three trajectories flown in the flight test are shown in figures 8(a), (b), and (c). For clarity, they will be referred to as passes 1, 2, and 3, respectively. The solid line shows the reference flight path, which includes the capture flight path in the track mode and the STOL approach route, and the dashed line indicates the flight path as estimated by the navigation system. The dotted line shows the fixed stored reference flight path. (The altitude profiles are discussed in a later section.) In the first two passes, the first target waypoint to be captured was waypoint 1, and in the third pass it was waypoint 2. For each pass, the system was taken out of track once. On returning to the predictive mode from the track mode, the waypoint to be captured is the next waypoint in the reference trajectory while the system was in track, unless otherwise selected by the pilot. In the first pass, the waypoint for reinitialization was waypoint 3. In the second pass, the waypoint during the path stretching maneuver was waypoint 2, and in the third pass, the waypoint after interrupting the track by a wind entry was waypoint 3.

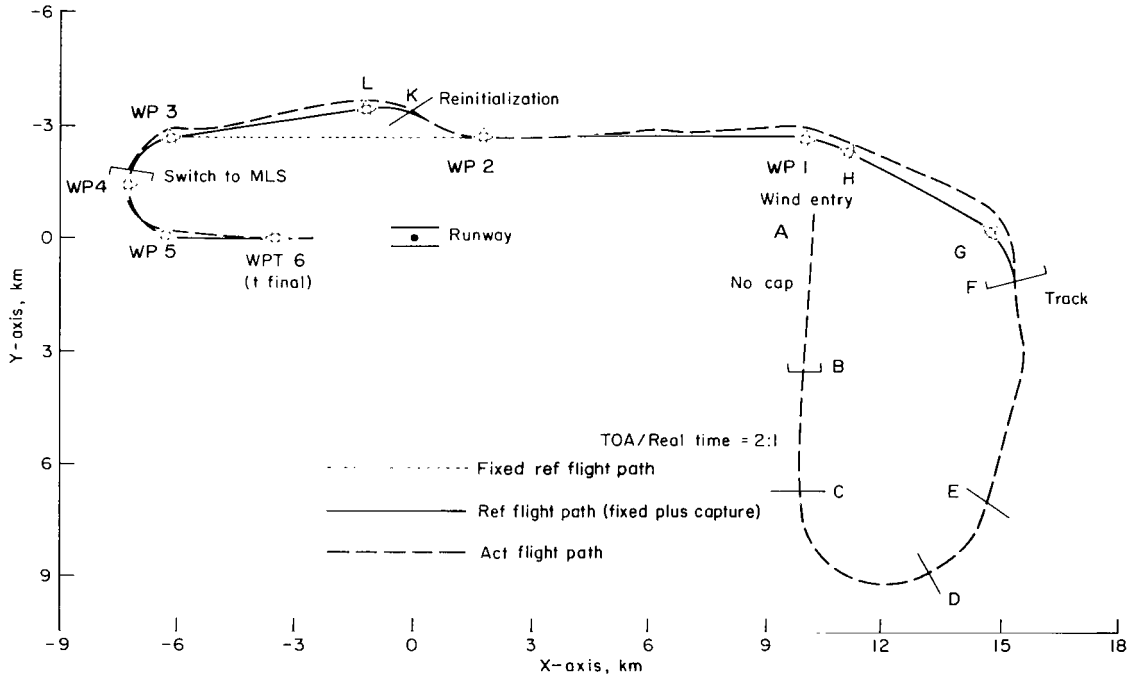

(a) Pass 1.

Figure 8.- Reference/actual flight path flown.

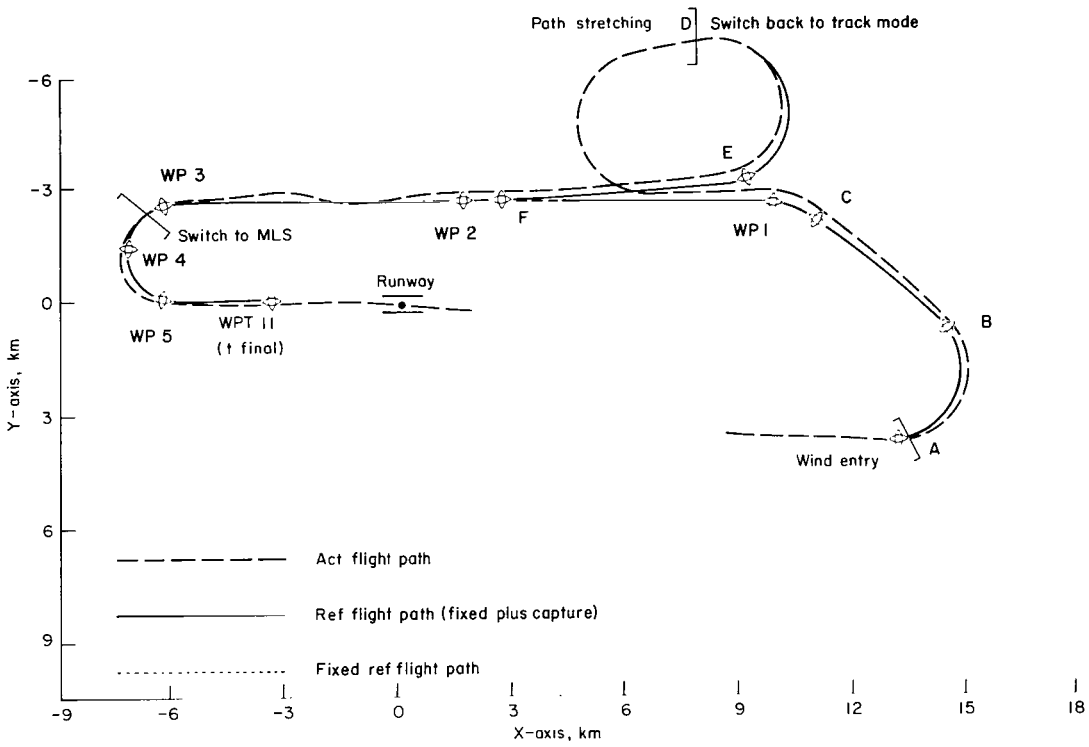

(b) Pass 2.

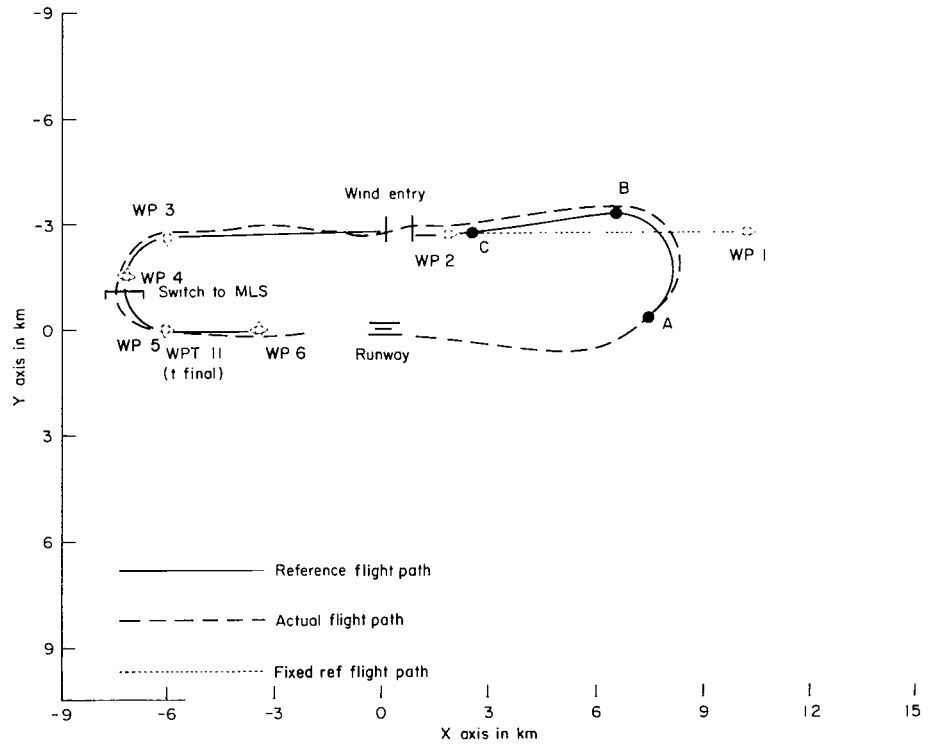

(c) Pass 3.

Figure 8.- Concluded.

The data recorded for events of the three passes is expressed as a function of Greenwich time. For the convenience of comparing corresponding data in different passes, a second time frame t (in sec) was also used. For purposes of a comparison in the latter, t was chosen so that it is equal to 650 sec at t_{final} for all three passes. This dual system of expressing time in either Greenwich time or t is used throughout the remainder of this report.

The first portion of the trajectory in pass 1 (fig. 8(a)) was flown in the predictive mode to determine the rate of TOA changes versus real time. From point A to point B, no capture trajectory was possible because of the closeness of the aircraft position to waypoint 1. From point B to C, TOA changed twice as fast as real time since the aircraft was flying away from the target waypoint. From point C to D, TOA changed approximately 1/5 as fast as real time since the aircraft was flying almost along the synthesized capture trajectory, even though the system was still in the predictive mode. From point D to E, TOA remained the same since the aircraft was flying exactly along the synthesized capture trajectory. At F, the system was placed into the track mode.

In the vicinity of waypoint 2, to exercise the reinitialization provision, the along-track and cross-track errors were deliberately allowed to build up, to an X (along-track) error of 1583 m and a Y (cross-track) error of 536 m, as defined in appendix A (fig. 21). The reinitialization process, which included placing the system out of track, synthesizing a capture trajectory to waypoint 3, and a new speed profile, returning the system to the track mode; computing a new TOA took only one second. Forty seconds later, the pilot adjusted the time of arrival to the original desired TOA by exercising the TDC command.

In the second pass (fig. 8(b)), the aircraft was required to delay its arrival time by 3 min while it was in the track mode. This delay time was beyond the range of shifting TOA by speed control alone and therefore path stretching was necessary. At 19:52:40 (t = 211 sec), halfway between waypoints 1 and 2, the pilot started to fly the aircraft away from the reference trajectory and initiated path stretching. Fifty seconds later (t = 261 sec), the system was switched to the predictive mode to observe the varying TOA, as displayed on the MFD. Twenty seconds later (t = 281 sec), the new desired TOA was on display and the pilot switched the system back to the track mode, resulting in a new TOA of within one second of the desired TOA. Ten seconds later, the pilot adjusted the time of arrival to the exact TOA by exercising the TDC command.

In the third pass (fig. 8(c)), the system was placed out of track by a wind entry at 20:04:44 (at t = 455 sec). Interrupted by the wind entry, the system switched immediately to the predictive mode and began to synthesize a capture trajectory to the next waypoint (in this case, waypoint 3). The system was then manually returned to the track mode. The whole process took 9 sec. Ten seconds later (or at t = 474 sec), the time of arrival was adjusted to the exact value of the previously specified TOA by exercising the TDC command.

In the remainder of this section, we focus our attention on the details of the navigation, guidance, and control data. The speed profiles are considered first; the synthesized ground speed profile and the reference airspeed profile, as generated in the control loop. We also give the wind profile as estimated by the navigation filter, and a time-history plot of the speed error, pitch error, and roll error as displayed on the EADI. In addition, we discuss the tracking accuracy, by giving a time history of the along-track, and cross-track, altitude, and heading errors.

Speed, wind, and altitude profiles- The reference airspeed Va(WPT), altitude Z(WPT), and the reference heading with respect to the runway centerline H(WPT), are specified at waypoints. Their numerical values are tabulated in table 1. The speeds are fixed for all passes. The ground speeds VQ(WPT) at these points are computed as the vector sum of the specified air speeds and the wind vectors W_{KB}. The wind vector is a keyboard entry. For speed profile calculations, the wind vector, after entry from the keyboard, was assumed to be constant until it was replaced by another constant wind vector from a keyboard entry. The numerical values of the reference ground speeds at waypoints and of the wind vector keyboard entries for all three passes are also given in table 1. As will be remembered, once during each pass the system was disengaged and placed back into the track mode. The heading 'Track' means the ground speed reference at the instant when the system is switched from the predictive mode back to the track mode. The reference ground speeds for corresponding waypoints for different passes are different, reflecting the different numerical values of the keyboard wind entries.

The specified ground speeds shown, together with the time sequence of acceleration commands, ΔT_i, $\dot{V}_i$(as shown in table 6, were used to generate the ground speed profiles $V_g(t)$ in the track mode via equations (A18) of the control law. The reference ground speed profiles for all three passes are shown in figure 9. The curves are labeled with waypoint symbols, numbers for the fixed path and letters for the capture flight path, to agree with the symbols on figure 8. When the aircraft was commanded to turn, there usually was a significant ground speed change. The linear reference ground speed change in a turn is designed to result in identical air speeds at the beginning and end of the turn, provided that the pilot-entered wind estimate was correct. Note, for instance, the following turns for pass 1, shown in figure 8(a). There is the initial turn F to G of the capture flight path, and also the two final half turns 3 to 4 and 4 to 5. Theoretically, having additional waypoints on the turn 3 to 5 (WPT 4) would minimize speed control activity, since the ground speed solution determines airspeeds at the waypoints. If WPT 4 had not existed, a linear ground speed change from the magnitude at WPT 3 to the magnitude at WPT 5 would have occurred.

The ground speed profiles generated in the above manner are used for TOA calculations. To meet the arrival time, the control system then uses the present wind estimate of the navigation system, rather than the pilot's wind entry at the keyboard, to convert the reference ground speed to a new reference airspeed $V_r(t)$ (eq.(A21)). This speed is then combined with several error feedback terms to result in a speed command $V_c(t)$ (eq.(A27)).

TABLE 1.- REFERENCE DATA

(a) Reference quantities specified at waypoints

	WPT 1	WPT 2	WPT 3	WPT 4	WPT 5	WPT 6
IAS (knots)	160	140	120	120	120	105
TAS in (m/sec)	86.5	75.2	64.9	64.9	64.9	55.6
Ref. ALT (m)	762	762	762	762	573	347.5
Heading with respect to runway centerline (deg)	180	180	180	90	0	0

(b) Reference ground speeds at waypoints in m/s

Pass	Track*	WPT 1	Track*	WPT 2	Track*	WPT 3	WPT 4	WPT 5	WPT 6
1	80.6	97.6		81.8	81.1	70.3	75.5	59.3	49.7
2	60.6	91	84.2	73.3		69.5	68.8	60.7	51.2
3			76.3	80.2	79.9	63.3	63.3	66.4	57.4

*Defined in the text.

(c) Keyboard Wind Entry

Pass	Time of entry (Greenwich)	At altitude (m)	Wind angle (deg)	Wind magnitude (m/sec)
1	19:35:41	1023	119	12.2
2	19:49:50	718.7	142	5.7
3	20:04:44	717.5	310	2.4

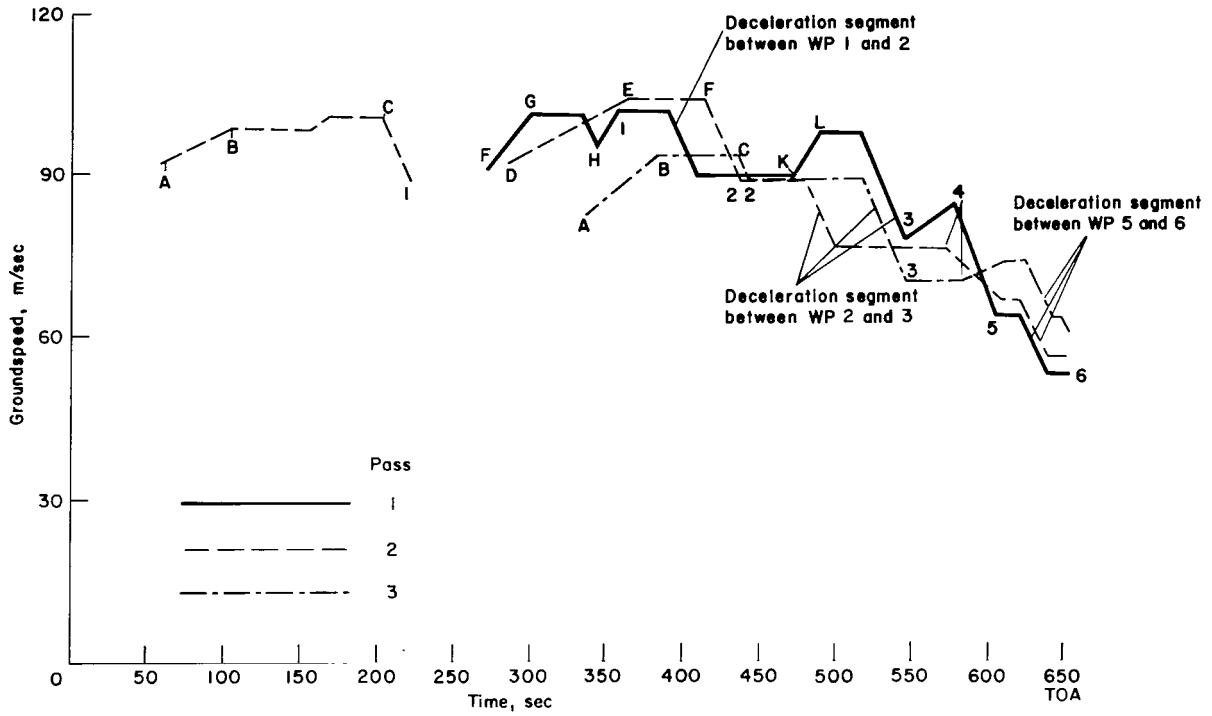

Figure 9.- Reference ground speed profiles March 5, 1974, flight.

Besides ground speed changes in turns, to preserve constant airspeed at the ends of the turns, there are also decelerations (fig. 9) required in the straight flight path segment to change speed from one waypoint to the next. It is not uncommon, therefore, for the resulting reference ground speed profile to contain a deceleration segment (for straight flight), followed immediately by an acceleration segment (for the turn) as shown at point H of the speed profile for the first pass.

The hills and valleys in the ground speed profile were expected to flatten out in the new reference airspeed profile $V_r(t)$ if the pilot-entered wind estimates agreed with the measured wind. Therefore, such changes should not cause concern since the new reference airspeed, and not the reference ground speed, was used to command the aircraft. Even if the pilot-entered wind was precisely equal to the measured wind and also to the actual wind, the linear ground speed change in the turns, designed to achieve proper airspeeds at the ends of the turns will cause small variations in the reference airspeed during the turns, because the theoretical ground speed variation for constant airspeed is not linear. The expected small variation in the new reference airspeed during the turn was based on the assumption that W_{kb}, the keyboard wind entry, would be in reasonable agreement with $W_{nf}(t)$, the actual wind vector measured. In other words, the magnitude and direction of the wind vector $W_{nf}(t)$ was assumed to be fairly constant, with only small variation about some constant value, which is approximately equal to that of the keyboard entry. The reference airspeed profiles for the three passes are shown in figure 10; the valleys and hills in the three curves did not flatten out as expected.

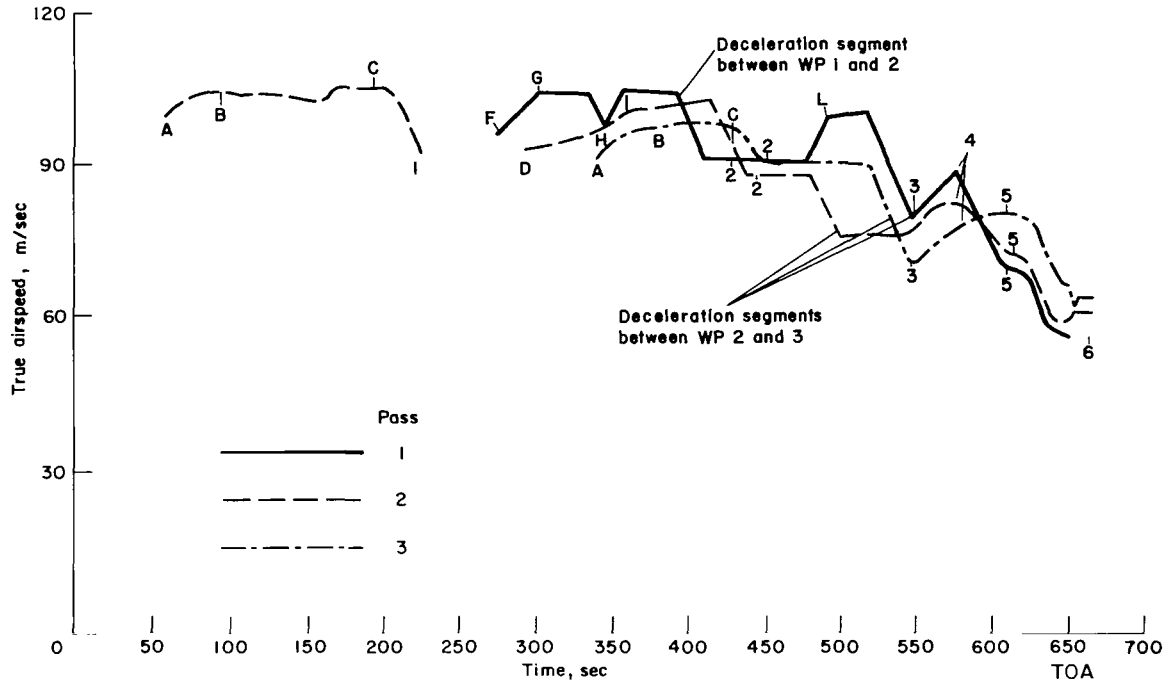

Figure 10.- Reference airspeed profiles March 5, 1974, flight.

The result will be explained by examining the wind profiles for the three passes. The wind magnitude and wind direction, as estimated from the navigation filter, and the altitude profile for the three passes are shown in figures 11(a), (b), and 12. The abscissa is the time t, which was so chosen that corresponding points in this axis correspond approximately, depending on the tracking accuracy, to the same spatial coordinates of the aircraft position, especially during the last two minutes (120 sec) before t final. Corresponding points in the t axis for the first and second passes are about 14 min apart in Greenwich time and for the second and third passes, exactly 8 min apart. Obviously, the wind estimate has large low frequency variations in both magnitude and direction. Before discussing the problems these variations cause in the speed control system, we first describe the measurement of the wind.

The ground speed components x_{nf}, y_{nf}, of the aircraft were computed from the complementary filters, having as inputs the estimated aircraft position computed from either TACAN or MODILS measurements and the processed output from vertical and directional gyros and from body-mounted accelerometers. The estimated wind was computed as the vector difference between the estimated ground velocity and the measured true airspeed, having x_A and y_A as its components. This wind estimate is then filtered in a 100-sec time-constant low-pass filter. From the detailed description of the navigation system given in reference 8 we know that the accuracy of ground speed estimated for MODILS has an rms value of 1.5 m/sec and for TACAN, 3 m/sec with low-frequency components present that will pass the wind filter.

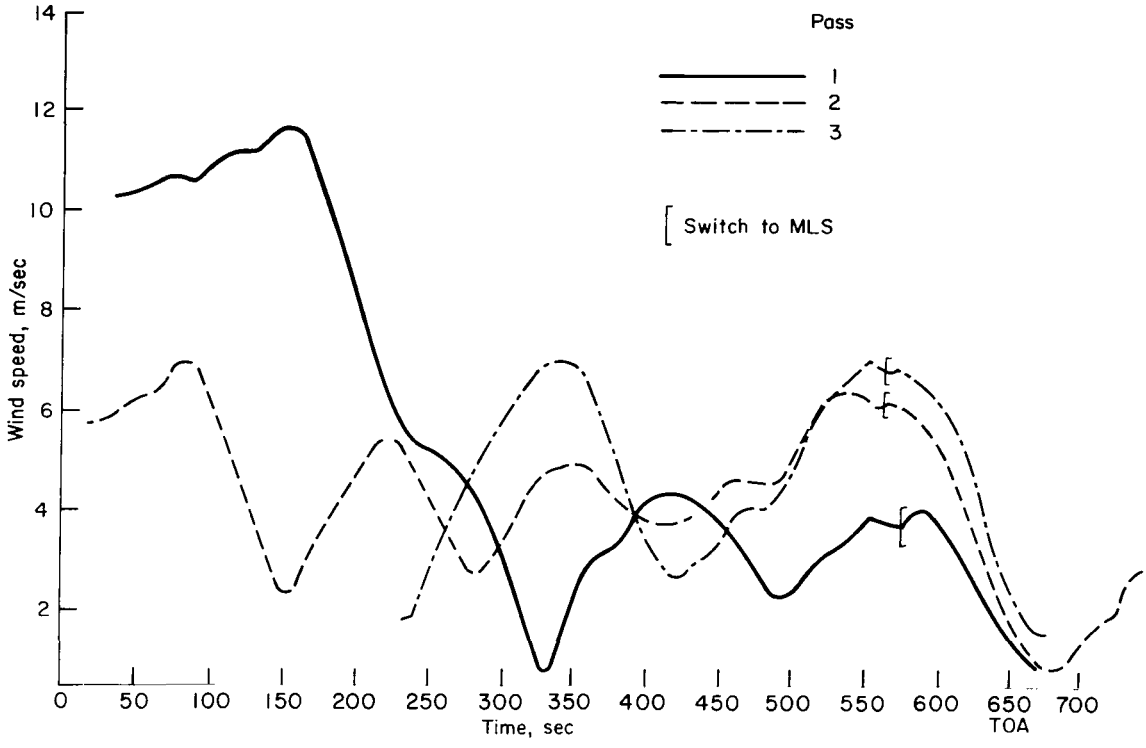

(a) Magnitude

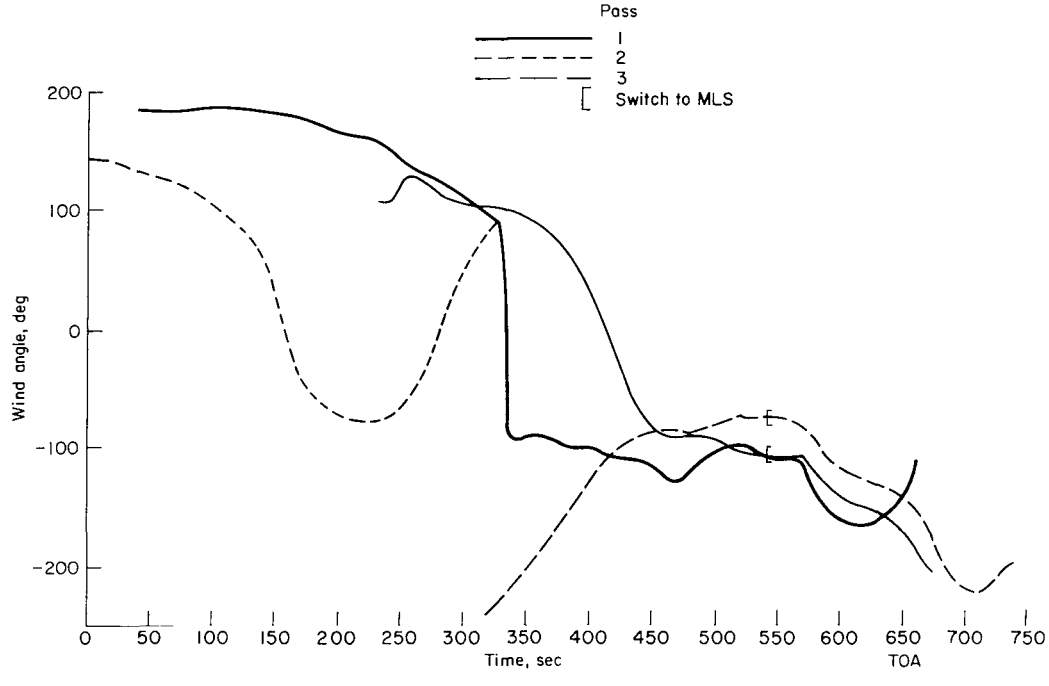

(b) Angle.

Figure 11.- Wind profile March 5, 1974, flight.

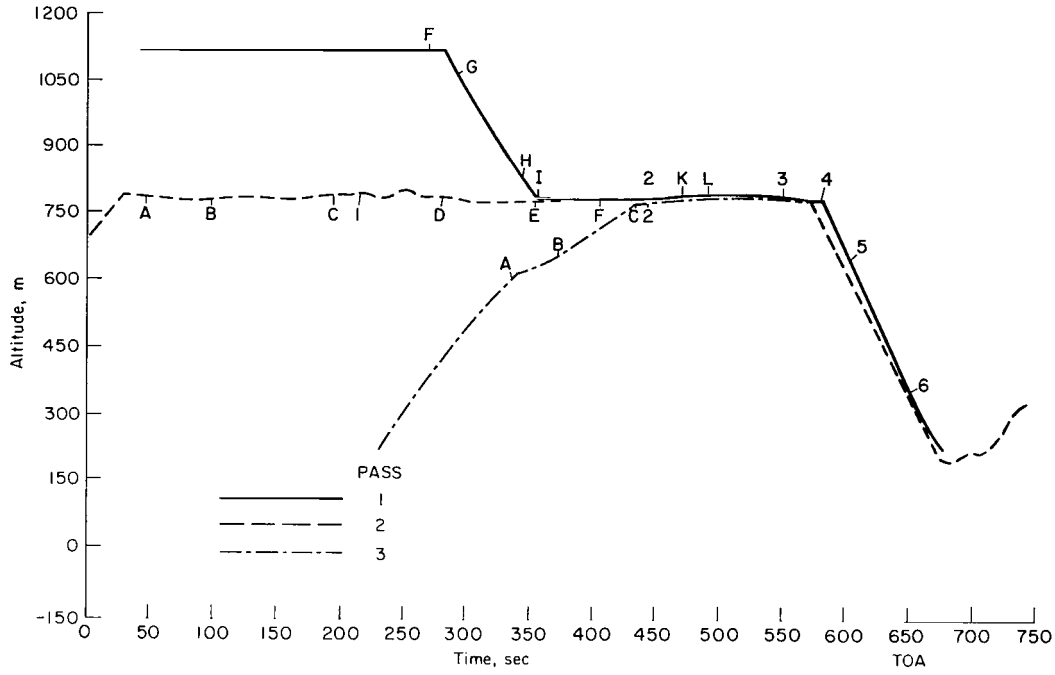

Figure 12.- Aircraft altitude profile March 5, 1974, flight.

As indicated in figure 12, the altitudes flown for the first 410 sec were quite different for each pass. It is known that wind magnitude and direction are strongly altitude dependent. Therefore, the wind estimates before 410 sec should not be compared with each other. Between 410 sec and the time to switch to MODILS the wind estimates remain within 3.6 m/sec of each other and the wind directions for the three passes remain reasonably constant and follow the same trend. At the time the system switches to MODILS the altitude is reduced also and the wind reduces. Decreasing wind with altitude is the usual trend. This effect can be seen for the descending portion of the first pass beginning at 290 sec, where the wind dropped almost to zero, while the direction changed very little, and then began to increase in the opposite direction. This is an almost constant gradient shear, which includes a zero wind layer. It should be noted, however, that while the aircraft is changing altitudes, the wind measurements contain large errors, since the altitude transition from 1100 to 750 m took place in 70 sec, while the low-pass wind filter had a time constant of 100 sec.

The statistics of the wind for the three passes and five simulated passes are shown in table 2. For the portions of flight at constant altitude, the wind magnitude for the three passes had standard deviations of 3.6, 1.8, and 1.8 m/sec, respectively. These figures compare with the ground speed estimation errors introduced in the wind estimate. Therefore, only a portion of these changes can be due to true atmospheric fluctuations. The magnitudes of the wind from keyboard entries are shown in the same table. The keyboard inputs were based on some instantaneous value of the wind estimate from the navigation filter. They differ from the average of the wind measured by a

TABLE 2.- WIND MAGNITUDE

Flight	Pass	Track mode	W_{kb}, m/sec	W_{nf}, m/sec			$W_{kb} - \bar{W}_{nf}$, m/sec
				Maximum	Average	Standard deviation	
Actual	1	Manual	12.2	12.3	5.4	3.6	6.8
	2	Manual	5.4	7.2	4.2	1.8	1.2
	3	Manual	2.4	7.2	4.5	1.8	-2.1
Simulated	1	Manual	0	1.8	0.9	0.4	-0.9
	2	Auto	12.8	13.3	12.4	.3	.4
	3	Manual	12.3	13.7	12.7	.5	-.4
	4	Auto	12.3	13.2	12.5	.7	-.2
	5	Auto	2.6	3.1	2.4	.5	.2

W_{kb} Wind from keyboard entry

W_{nf} Wind estimated from navigation filter } for the constant altitude portion of the flight paths.

$\bar{W}_{nf}$ Average W_{nf} }

large amount in the first pass, and by a substantial amount in the second and third passes. The large difference in the first pass is attributable to the keyboard wind entry at a much higher altitude, where the estimated wind magnitude was much larger.

Table 2 also gives the statistics of the wind for five simulated flights, where the simulated wind remains constant at the tabulated values, but the estimated wind contains errors due to navigation errors. The simulated flight was conducted to supplement the actual flight results so that the tracking accuracy of the simulated and actual flights can be compared. One comparison is the system performance in the automatic tracking versus manual tracking. The second comparison is to determine the effects on the guidance of large wind estimation errors in actual flight versus small errors in the simulated flights.

Two of the simulated flights were made in the manual tracking mode and three in the automatic tracking mode. In the manual tracking mode, one pass was conducted with zero wind input and the other with a 12.3 m/sec wind input from the keyboard. In the automatic tracking mode, two passes were flown with large keyboard wind input (i.e., 12.8 m/sec and 12.3 m/sec, respectively), and the third pass with a wind entry of 2.6 m/sec. In each case, the keyboard entry equals to the wind that was simulated.

The reference airspeed $V_r(t)$, already shown in figure 10, the commanded airspeed $V_c(t)$, which includes the feedback term in equation (A27), and the actual airspeed $V_a(t)$ are shown in figures 13(a), (b), and (c) for passes 1,

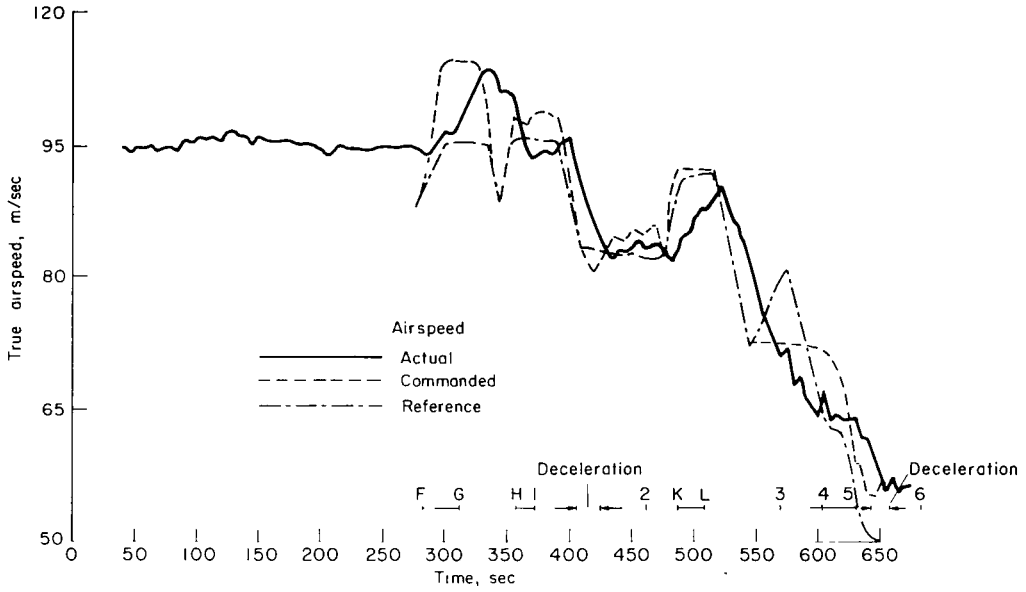

(a) Pass 1.

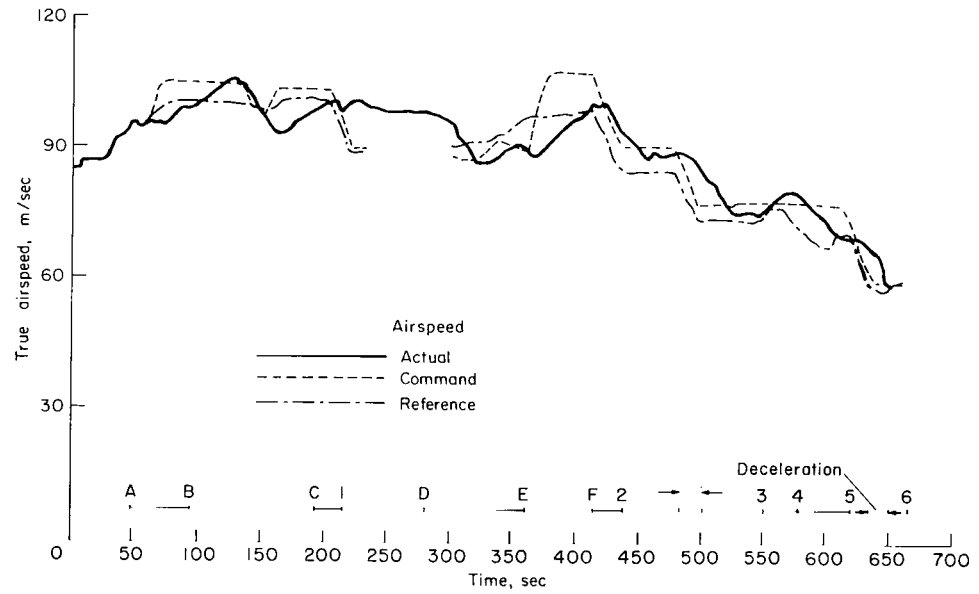

(b) Pass 2.

Figure 13.- Actual, commanded, reference airspeed profile for March 5, 1974, flight.

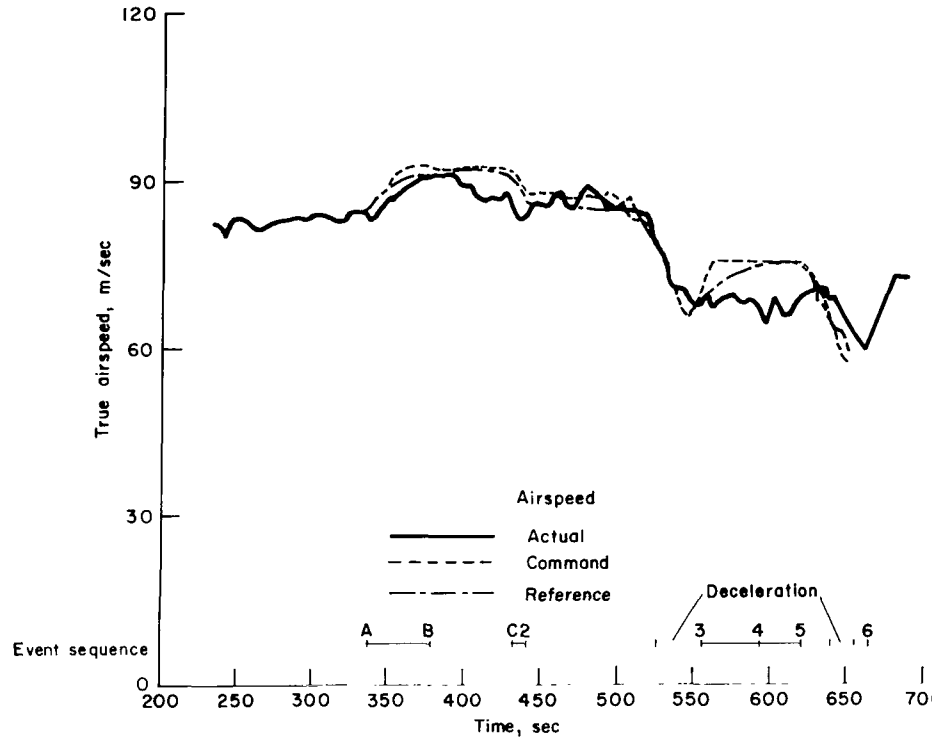

(c) Pass 3.

Figure 13.- Concluded.

2, and 3, respectively. The change in wind speed estimate with time and the method of using this estimate given in equation (A20) for airspeed command calculations caused large command fluctuations. In fact, it was often limited by the various constraints discussed in the appendix. The actual airspeed did not follow the commanded airspeed too closely.

Flight director command bar histories- The difference between the actual and the commanded airspeed were used to drive the speed command bar of the EADI for manual tracking. A time-history plot of the speed error bar deflection for the three passes is shown in figures 14(a), (b), and (c), respectively, together with flight path angle and roll error. The speed error curves indicate large fluctuations in the speed error throughout the flight, especially in the first two passes.

The pitch and roll command errors, after passing through their respective position and rate limiters, generate deflections of the pitch flight director bar of 0.254 cm/deg and the roll flight director bar of 0.1 cm/deg. From the relative deviations of the curves in figure 14, it appears that, in manual flight, the pilot assigned a hierarchy of importance to these three control variables, which (in descending order) are pitch angle, bank angle, and speed. As shown later, the hierarchy is reflected also on the magnitude of the errors in altitude, in heading and in along-track and cross-track error. The altitude error was the smallest and the along-track and cross-track errors were the largest.

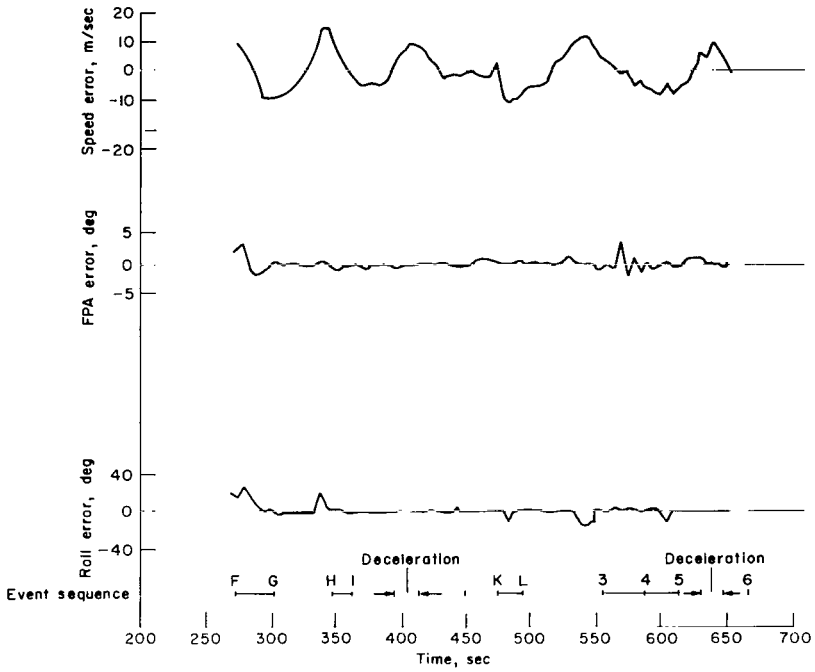

(a) Pass 1.

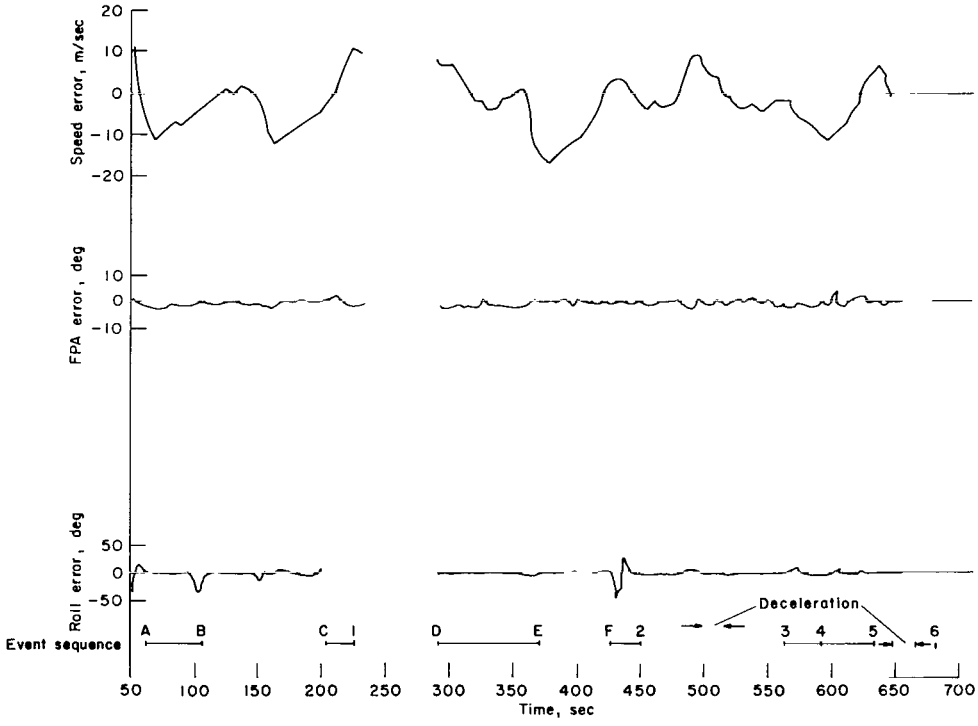

(b) Pass 2.

Figure 14.- Speed, FPA, rool error for March 5, 1974, flight.

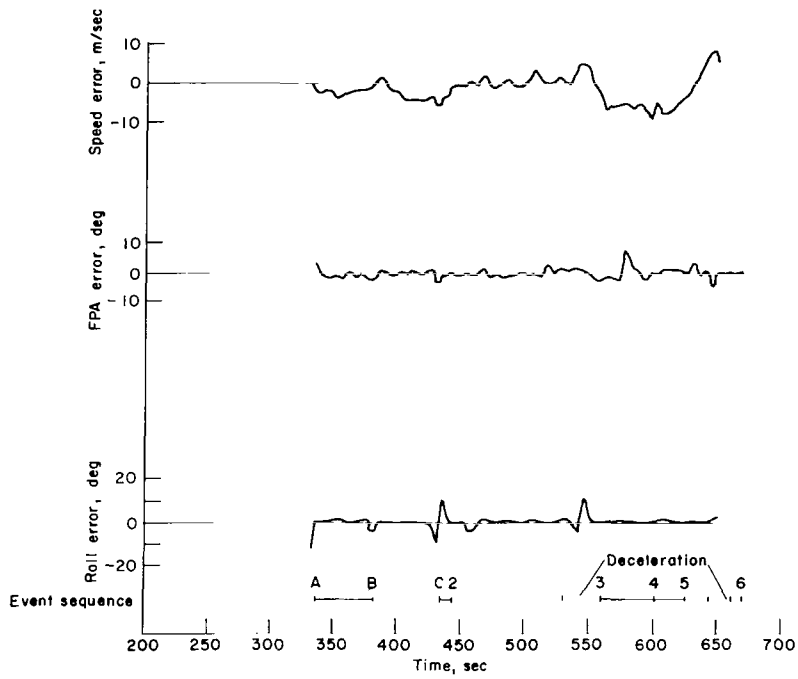

(c) Pass 3.

Figure 14.- Concluded.

Guidance errors- The along-track and cross-track guidance errors for the flight are shown in figures 15(a) and (b), respectively. Event markers have been drawn to permit correlation with changes in the flight path as shown on figure 8. Navigation errors or total errors are not discussed, because precision radar tracking was not available for the flight.

The statistics of the guidance altitude errors are shown in table 3. The along-track error has an average of -127.7, -134.7, and -139 m for the three passes, meaning that the aircraft was behind the phantom by more than 120 m most of the time. This lag occurred mostly during turns (fig. 15(a)), when the pilot workload is especially high, and when the pilot is asked in addition to accelerate the aircraft. The cross-track error has an average of 127.7, 149.6, and 174.0 m for the three passes respectively, meaning the aircraft was to the right of the phantom most of the time (fig. 15(b)). This standoff error in y was due to an error in measuring the aircraft heading ψ_A and is a function of the control law (A28). It was discovered in the postflight analysis in a comparison of the heading as determined from the navigation filter velocities ($\arctan(\dot{y}/\dot{x})$) corrected for the drift angle with the heading gyro output. This analysis is valid, since during straight flight, the headings calculated from the navigation filter velocity estimates are not sensitive to heading gyro error. The average error in measuring this angle was about 5.5°. Substituting this number into equations (A26) and (A28) results in an average offset error of approximately 152.4 m in y. Therefore, the offset error is consistent with the error in the heading measurement.

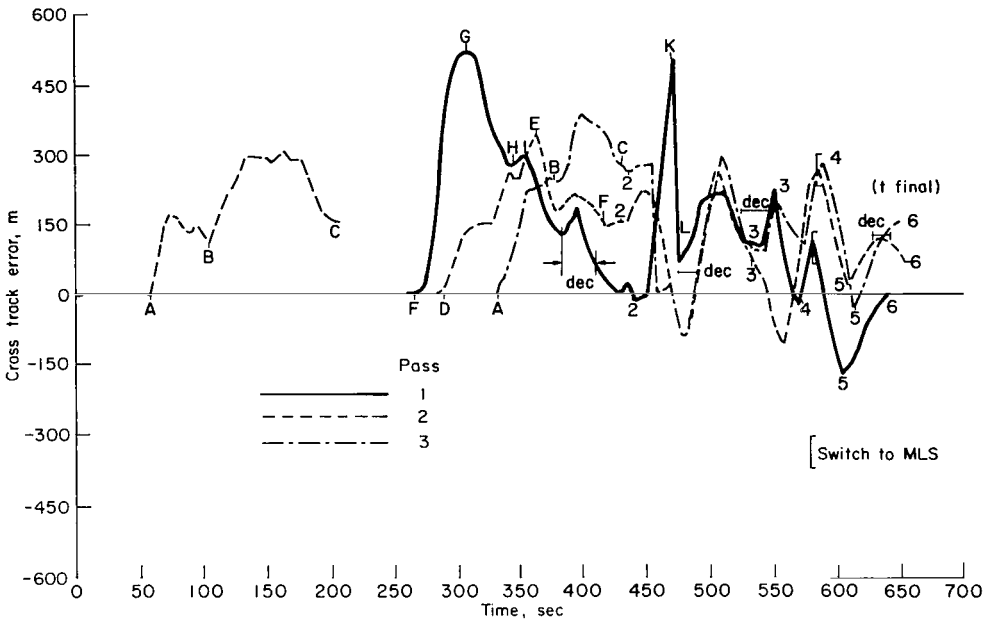

(a) Along-track.

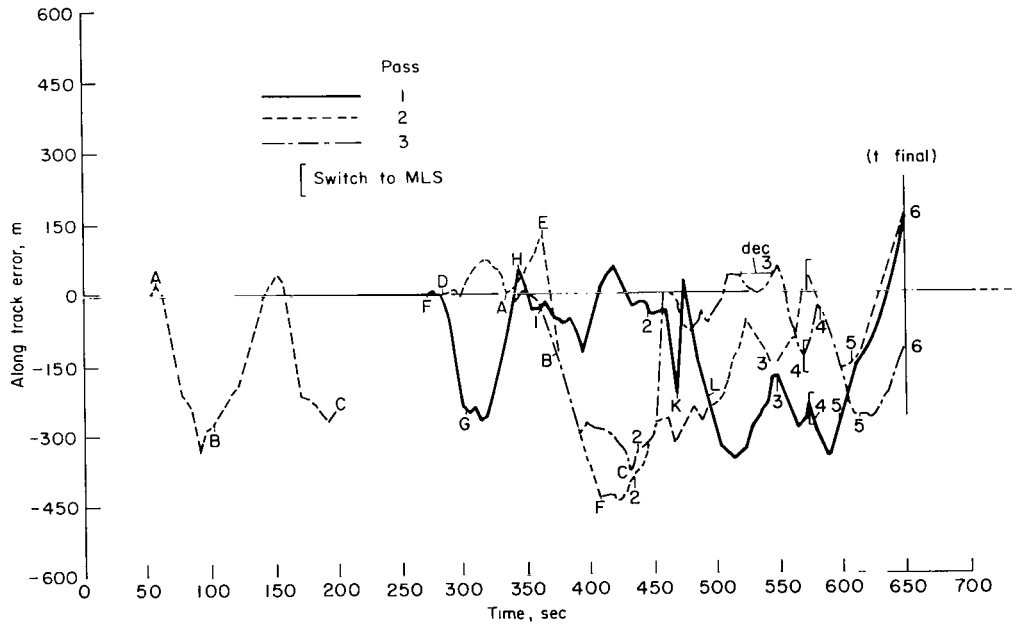

(b) Cross-track.

Figure 15.- Guidance errors March 5, 1974 flight.

TABLE 3.- GUIDANCE ERRORS

Pass		Track mode	Along-track error, m		Cross-track error, m		Altitude error, m	
			Average	Standard deviation	Average	Standard deviation	Average	Standard deviation
Actual flight	1	Manual	-127.7	130.1	127.7	161.2	-1.6	6.4
	2	Manual	-134.7	145.0	149.6	96.6	-2.0	3.9
	3	Manual	-139.0	121.3	174.0	110.3	-0.70	4.5
Simulated flight	1	Manual	-21.0	32.9	-1.8	25.6	-.85	3.6
	2	Auto	-10.0	19.8	0.61	18.2	.52	2.7
	3	Manual	-25.9	26.2	-7.6	24.3	-.15	3.3
	4	Auto	-7.3	32.0	2.9	14.0	-.06	2.4
	5	Auto	3.0	46.9	4.5	12.2	-.61	2.4

The average altitude guidance error for the three passes is less than 3 m and the maximum altitude error is less than 30 m. The standard deviation of the altitude error is one order of magnitude less than that of the error in horizontal position.

The simulated flight includes both manual and automatic tracking modes, as well as different wind conditions (the wind magnitude for the simulation ranged from 0 m/sec to 12.8 m/sec in the five passes, table 2). As shown in table 3, the average along-track error for the automatic tracking mode is about half that of the manual tracking. The wind magnitude has no apparent effect on the tracking accuracy. It should be remembered that the automatic tracking mode is not fully automatic since the flap must be deployed manually. Therefore, the along-track accuracy is quite sensitive to the proficiency of flap deployment. For this reason, the time control in the automatic mode was not better than the manual mode.

The average cross-track error in the simulated flight is practically zero and the standard deviation is 1/4 of that for the actual flight. The tracking accuracy for the altitude channel is about the same for both the actual and the simulated flight.

Errors at the approach gate- At the approach gate, the along-track, cross-track, altitude, heading, and TOA errors for the three passes are shown in table 4. The maximum TOA error is less than 3-1/2 sec, which is 3484 m from the runway and 305 m above it.

Table 4 also shows errors at the approach gate for the simulated flights. The along-track errors at the gate are a small fraction of those for the actual flight, with the exception of pass 5, in which the flap was deployed too late and the aircraft was not given the required time to decelerate, thus causing a large along-track error at the gate. The cross-track error for the

TABLE 4.- ERRORS AT THE APPROACH GATE

Flight	Pass	Track mode	Along-track error, m	Cross-track error, m	Altitude error, m	Heading error, deg	TOA error, sec
Actual	1	Manual	172.2	20.4	12.5	-1	3.1
	2	Manual	174.0	68.3	11.0	-6	3.2
	3	Manual	-97.8	140.8	7.0	-6	-1.6
Simulated	1	Manual	-7.3	-2.1	0.6	0	-0.2
	2	Auto	28.9	9.1	14.6	-8	.5
	3	Manual	17.0	13.7	5.8	-3	.3
	4	Auto	19.2	19.5	13.7	-3	.4
	5	Auto	76.2	12.5	17.7	-1	1.4

simulated flight is again a small fraction of that for the actual flight. The altitude error at the gate is about the same for both the actual and simulated flights. The TOA, strongly dependent on the along-track error at the gate, is much better in the simulated flight as compared with the actual flight. Except for pass 5, the maximum TOA error is at most 0.5 sec.

The main differences between the actual and simulated flights are the degree of uncertainty of the wind and the navigation errors. The simulated flight results provide us with the limit to which the tracking errors can be reduced.

PILOT ACCEPTANCE

Although the flight test environment was not fully representative of an operational situation (e.g., single aircraft ATC simulation and visual flight conditions), the pilot felt the system has the potential for being acceptable in an operational environment. Some specific observations were:

1. Arriving at the specified time of arrival was an easy task. It was easy to adjust the initial flight path to allow 4D engagement such that the specified TOA was made. TOA adjustments subsequent to 4D engagement were also easily accomplished.

2. The workload associated with controlling the longitudinal and lateral flight director was quite low, allowing adequate time to monitor the progress

of the flight. Some compensation was required for speed control as the speed error bar seemed excessively noisy.

3. The STOLAND displays (EADI, MFD, HSI, and status panel) permitted the progress of the flight to be easily monitored. The map display on the MFD is particularly useful for a quick assessment of situation data.

4. Since the system has several simplifications in it, the pilot must keep the aircraft fairly close to the reference or phantom aircraft position or the flight director commands can become meaningless. This was initially a problem, but after a short learning period the pilot learned how much error could be developed without causing problems. This was no problem in the flight test program, but operationally in an abuse situation (e.g., an inflight emergency requiring the pilots attention) it could lead to a situation where 4D guidance is no longer possible.

CONCLUSIONS

The 4D RNAV system concept described in this report has demonstrated the capability of providing the pilot a capture flight path to a reference flight path which was computed from waypoints assigned by ATC. The system informs the pilot immediately whether a capture flight path is within the capability of the aircraft. The capture flight path concept, which is one of the unique contributions to 4D RNAV, makes it possible for the pilot to respond quickly and efficiently to ATC instructions.

In terminal area RNAV problems, where 4D is started within 50 n.mi. of the landing field, the time spent on the capture flight path is an appreciable portion of the total flight path to landing. In this case, the capture flight path and algorithm to compute it are essential to any 4D RNAV system for predicting and achieving a specified time at the final waypoint. In all cases, including point-to-point flight paths, the capture flight path concept permits alteration of routes and path stretching or shortening to accomplish changes in ATC objectives. To make this feature applicable for 4D application, however, coupling to a specific capture flight path, while being able to examine alternate routes via tentative predictive capture flight paths, would be desirable.

The conclusions must be qualified by the following limitations of the tests:

1. The tests were conducted by a test pilot, who was familiar with the system.

2. Data input to the keyboard was performed by a helper, to whom the pilot called out the required inputs.

3. ATC commands were simulated by the test conductor.

4. Other air traffic was minimal during the flight test.

5. No system failures were considered.

6. The test was carried out in VFR conditions.

7. Winds varied, but were not excessive.

The simulator tests, which included the STOLAND avionics hardware, have shown that the pilot displays and controls were adequate to permit the pilot to monitor the system's performance in the automatic mode, or to guide the airplane via flight director commands although failure modes have not been studied. The accuracy of controlling aircraft position and speed to achieve a specified time-of-arrival was adequate according to the standards set in references 5 and 6. Automatic computation, recomputation, and display of a time-controlled capture trajectory from the present location of the aircraft to a selected waypoint on the reference trajectory, while the system is in the predictive mode, was shown to be useful in determining and controling TOA. The capture trajectory concept also proved useful for path-stretching purposes to delay the TOA to a specified time. Considering the task, which could not have been performed with any precision without a 4D system, the workload was moderate for both automatic and manual systems. However, in the flight director mode, it was essential to control speed fairly tightly in order for the path control system to work properly, which at least for the present system increased the workload significantly.

The flight test confirmed the findings of the simulator tests, but it also revealed deficiencies, which must be avoided for operational systems. Since the system was originally designed for automatic control only, along-track and cross-track controls were coupled via a linear set of control laws. This meant that speed and roll control were equally critical for precise path tracking and both had to be performed with precision for the flight director commands to remain meaningful. This increased the workload compared to another technique that has been flight tested at Ames Research Center (ref. 9), in which cross-track and along-track controls are independent of each other. Also, the linear horizontal flight path tracking control law was sensitive to heading gyro errors as well as wind estimation errors. This problem can be avoided by feeding back only the cross-track velocity and position as obtained from the navigation filter outputs. As noted, in straight flight, the navigation filters are insensitive to small gyro bias errors. Also the control law of reference 9 is wind proof, since it involves inertial quantities only. Finally, the reference airspeed was too sensitive to the wind estimation errors. Winds do vary significantly with time and altitude in magnitude and direction. Wind estimates are the result of heavily filtered estimates based on the difference of two noisy almost equal quantities, ground speed and airspeed. The wind speed estimate, therefore, should not appear directly in a speed command. In the manual mode, however, the pilot did not close the along-track loop tightly and therefore avoided throttle activity at a small cost in time control. This technique should also be used in the automatic system, although design details are not clear at this time. It is concluded that automatic speed control for 4D RNAV without excessive throttle activity and unnecessary speed changes should receive emphasis in future research.

The acceptability of 4D RNAV to the pilot depends on the ease with which the pilot can communicate with the ATC and direct the system to respond, and the manner in which the ATC and aircraft situations are displayed to him. Pilot evaluation of the system has shown that through the use of digital logic and advanced electronic displays, the algorithms and display formats that have been derived and are presented herein make 4D RNAV predictive guidance a concept that appears to have the potential for an operational system.

Ames Research Center
National Aeronautics and Space Administration
Moffett Field, Calif., 94035, May 7, 1975

APPENDIX A

4D RNAV EQUATIONS AND LOGIC IMPLEMENTED IN THE EXPERIMENTAL FLIGHT SYSTEM

The basic 4D system is described in references 1-4. In the flight system, simplifications had to be made, and realistic restrictions had to be added. This appendix addresses portions of the 4D RNAV system that differ from those described in the above references. The executive algorithm, an implementation of the logic for executing various algorithms designed for this system, which has never been reported, is also described. The purpose of the system description is to provide a background of how the 4D RNAV equations and logic were implemented in the airborne digital computer.

Reference Flight Path

The reference flight path is specified by a number of waypoints, each specified by the type of waypoint, its position coordinates, the desired turning radius, and the desired airspeed. There are two types of waypoints, a type 0 for unspecified final heading and a type 1 for specified heading. In figures 16(a) and (b), the solid dots and the arrow are the specified elements of the waypoint.

Trajectory synthesis is accomplished in four steps. First, the horizontal flight path is synthesized between consecutive waypoints, starting from the last to the first, the last being the approach gate. This order is necessary since the aircraft heading is assumed to line up with the runway at the gate. The synthesized horizontal flight path for type 1 waypoints takes the form of a straight flight-turn and for type 0, straight flight-turn-straight flight (see figs. 16(a) and (b)). The dotted lines and circles indicate some of the geometrical construction and auxiliary points that must be computed (ref. 4). The overall horizontal flight path is formed by a concatenation of horizontal flight path segments synthesized for consecutive waypoints.

Second, a vertical profile is synthesized by calculating the flight path angle from the difference in altitude divided by the total horizontal path length between waypoints:

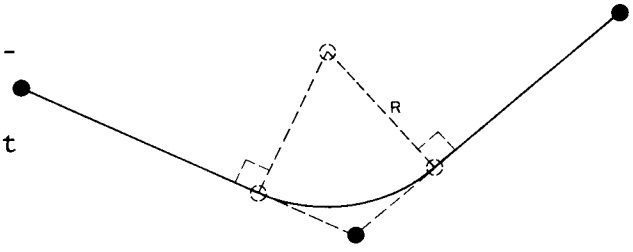

(a) Type 0 waypoint.

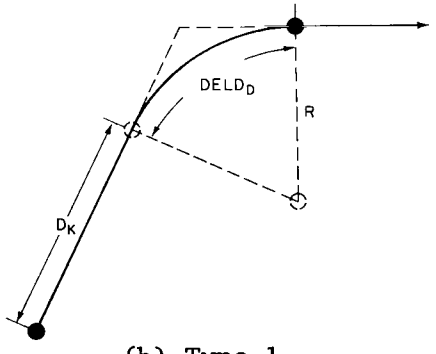

(b) Type 1.

Figure 16.— Waypoint definition.

$$\gamma_k = \tan^{-1}\left[\frac{-\left(ZWP_k - ZWP_{k-1}\right)}{D_k + DELD_k}\right] \tag{A1}$$

where γ_k is the flight path angle; ZWP_k the z coordinate of the waypoint; D_k and $DELD_k$ the horizontal distance substended by the straight flight and turn, respectively; and k the subscript for waypoint k.

Third, we synthesize the ground speed profile by concatenation of profile segments. A profile segment is the ground speed profile for a straight-flight turn horizontal flight path of figure 16(b) (see also fig. 17). This is independent of the types of waypoints that originally specified the flight path path. If the flight path is of sufficient length, the speed profile for the straight-flight portion consists of three speed segments; a constant speed segment at VQ_{k-1}, a deceleration segment from VQ_{k-1} to VP_k, and another constant speed segment at VP_k. The ground speed profile for the turn, shown shaded in figure 17, consists of a linear speed change from VP_k to VQ_k. The

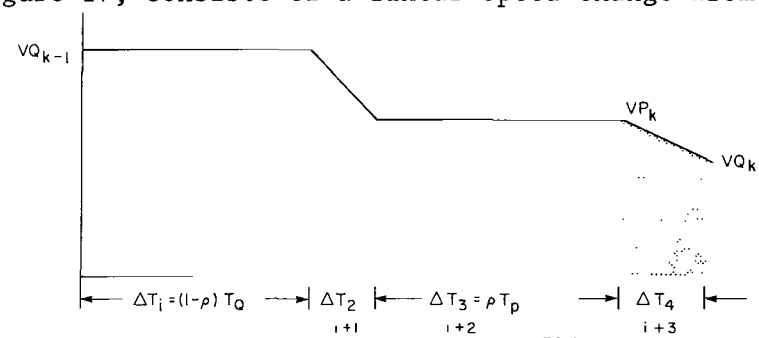

(a) Nominal profile.

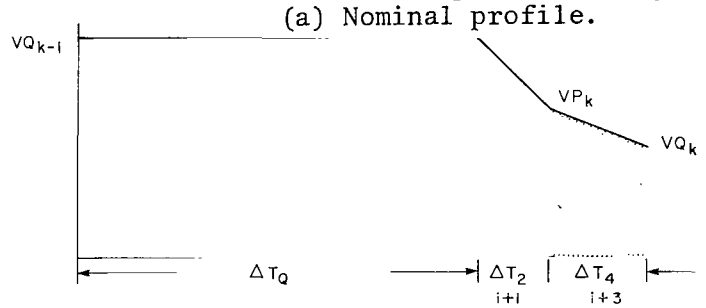

(b) Minimum TOA profile.

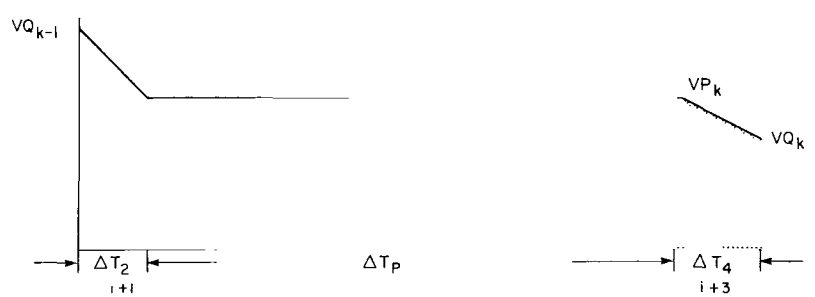

(c) Maximum TOA profile.

Figure 17.— Segment of speed profile.

ground speeds change so that the air speeds at the beginning and the end of the turn will be the same, provided that the pilot-entered wind speed estimate is equal to the actual wind.

The three-segment speed profile between waypoints provides the capability of adjusting the speed for advancing/delaying TOA. The two extreme cases are depicted in figures 17(b) and (c), the speed profiles for minimum and maximum time of arrival respectively. The minimum TOA profile corresponds to flying at the higher speed as long as possible (or, equivalently, decelerating as late as possible), and the maximum TOA profile, flying at the lower speed as long as possible (or decelerating as early as possible). In these figures, the shaded area under the curves represents the distance $DELD_k$, and the unshaded area under the curve represents the distance D_k (fig. 16(b)). Relations for computing the appropriate ground speeds and the time duration for the speed profile are given in equations (A2) through (A8). Ground speed is computed from airspeed VA_k and wind estimates, (EWMAG, EWANGL) as follows:

$$VP_k = VA_k + EWMAG^* \cos(H_k - EWANGL) \tag{A2}$$

$$VQ_k = VA_k + EWMAG^* \cos(H_{k+1} - EWANGL) \tag{A3}$$

distance to decelerate from VQ_{k-1} to VP_k;

$$VDIST = \frac{VQ_{k-1}^2 - VP_k^2}{2A} \tag{A4}$$

time duration for high speed segment

$$\Delta t_i = (1 - \rho) \frac{(D_k - VDIST)}{VQ_{k-1}} = (1 - \rho)\Delta T_Q \tag{A5}$$

time to decelerate

$$\Delta t_{i+1} = \frac{VDIST}{2(VQ_{k-1} - VP_k)} \tag{A6}$$

time duration for low speed segment

$$\Delta t_{i+2} = \rho \frac{(D_k - VDIST)}{VP_K} \rho(\Delta T_P) \tag{A7}$$

and time to turn

$$\Delta t_{i+3} = \frac{DELD_k}{(VP_k + VQ_k)/2} \tag{A8}$$

where VP, VQ are the ground speed at the beginning and end of a turn, respectively; VA the specific airspeed; EWMAG, EWANGL the estimated wind

magnitude and direction; H the reference aircraft heading generated in step 1; VDIST the horizontal distance traversed while the aircraft decelerates from VQ_{k-1} to VP_k; and A the nominal acceleration. The index ρ is used for adjusting the TOA in flight. For $\rho = 1$, the duration for the first segment is zero, corresponding to maximum time delay. Similarly for $\rho = 0$, the duration for the third segment is zero, corresponding to arriving at the gate as early as possible. Finally, five arrays for time control and a command table are generated. They are $TMAX_k$, $TMIN_k$, $ENRTIM_k$, the maximum, minimum, nominal time required to fly the aircraft from waypoint k to the approach gate; and $TSHIFA_k$, $TSHIFD_k$, the time available for advancing and delaying TOA at waypoint k. The nominal time $ENRTIM_k$ is set equal to half way between $TMAX_k$ and $TIMN_k$ to allow the pilot equal flexibility in adjusting TOA. These five arrays are computed by equation (A9) through (A13).

$$TMAX_k = \sum_{j=k}^{NWP} (\Delta T_2 + \Delta T_P + \Delta T_4) \tag{A9}$$

$$TMIN_k = \sum_{j=k}^{NWP} (\Delta T_Q + \Delta T_2 + \Delta T_4) \tag{A10}$$

$$ENRTIM_k = \sum_{j=k}^{NWP} (1 - \rho)\Delta T_Q + \Delta T_2 + \rho \Delta T_P + \Delta T_4 \tag{A11}$$

$$\begin{aligned} TSHIFA_k &= TMIN_k - ENRTIM_k \\ &= \sum_{j=k}^{NWP} (D_j - VDIST)\left(\frac{1}{VQ_{j-1}} - \frac{1}{VP_j}\right) \end{aligned} \tag{A12}$$

$$\begin{aligned} TSHIFD_k &= TMAX_k - ENRTIM_k \\ &= (1 - \rho) \sum_{j=k}^{NWP} (D_j - VDIST_j) \left(\frac{1}{VQ_{j-1}} + \frac{1}{VP_j}\right) \end{aligned} \tag{A13}$$

The command table, consisting of our arrays — that is, the time duration for executing the commands Δt, the ground acceleration command $\dot{V}$, the turning radius R, and the inertial flight path angle γ — is generated by the following relations,

$$\left.\begin{array}{llll} \Delta t_i = \Delta T_i & \dot{V}_i = 0 & R_i = 0 & \gamma_i = \gamma_k \\ \Delta t_{i+1} = \Delta T_{i+1} & \dot{V}_{i+1} = A & R_{i+1} = 0 & \gamma_{i+1} = \gamma_k \\ \Delta t_{i+2} + \Delta T_{i+2} & \dot{V}_{i+2} = 0 & R_{i+2} = 0 & \gamma_{i+3} = \gamma_k \\ \Delta t_{i+3} = \Delta T_{i+3} & \dot{V}_{i+3} = \dfrac{VQ_k - VP_k}{\Delta T_{i+3}} & R_{i+3} = R_k & \gamma_{i+4} = \gamma_k \end{array}\right\} \tag{A14}$$

Synthesized Reference Flight Path

The reference flight path that was actually flown in this flight test will be derived as an example. The inputs to the preflight synthesis program, consisting of the type of waypoint, the specified coordinates for the waypoints (XWP, YWP, ZWP), the turning radius and the indicated airspeed, are given in table 5. The outputs from the synthesis program, consisting of a table of commands and the time gate (maximum minus minimum possible flight times) for arrival at the final waypoint, are shown in table 6. Each line represents a path change in turn, acceleration, or flight path angle. The synthesized horizontal flight path and the vertical profile are shown in figure 1. At the pilot's option, the capture flight path may be connected to any of the specified waypoints, except the final waypoint.

The reference flight path was designed to have two relatively long segments, which include deceleration maneuvers. This permits a maximum adjustment of arrival time by shifting the points of deceleration. In this experimental system, deceleration was restricted to occur between adjacent waypoints in order to achieve computational efficiency and simplicity. The third deceleration to the landing airspeed of 105 knots is done in the final straight-in glide-slope segment as landing flaps are deployed. The control system will command 105 knots of IAS at the final waypoint even if a time error exists. The 5° glide slope is started halfway around the turn on the final leg of the approach path. In terms of turn radius and glide slope, this path is similar to that flown earlier with another 4D system (ref. 9), thus permitting comparison of flight test results.

Capture flight path— The capture flight path provides a flyable path from the present aircraft position and heading to those of a pilot-selected waypoint. It is a minimum-length flight path, which is therefore unique, and allows the pilot the largest range in choice of time of arrival. The general problem of minimum length flight paths has been treated in reference 10, but has been simplified for airborne implementation (ref. 4).

The horizontal capture flight path, consisting of a turn-straight flight turn, is synthesized by the following iterative process:

1. Compute a turn-straight flight path from the current aircraft position P_a and heading H_a to the selected waypoint WPT_k (fig. 18(a)), thus generating point Q.

2. Compute a straight flight-turn path from Q to the specified waypoint WPT_k and heading H_{k+1}, thus generating the point P (fig. 18(b)); note that line P - Q is not tangent to the circle P_A - Q.

3. Compute a turn-straight flight path from P_a, H_a to P (fig. 18(c)); note that now P - Q is not tangent to the circle P - WPT_k.

4. Ascertain if the -HH1, the negative of the heading generated in step 2 (fig. 18(b)) and HWP, the heading generated in step 3 (fig. 18(c)) are

TABLE 5.— INPUT TO PREFLIGHT SYNTHESIS PROGRAM

Waypoint	WPT type	WPT coordinates, m			Turning[a] radius, m	KIAS, knots
		XWP	YWP	ZWP[b]		
1	1	9780	-2743	-719	0	160
2	1	1849	-2743	-719	0	140
3	1	-6078	-2743	-719	0	120
4	1	-7440	-1371	-719	1371	120
5	1	-6078	0	-531	1371	120
6	1	-3484	0	-305	0	105

[a]Positive for right turn, negative for left turn, zero for straight flight.
[b]Above runway, runway at altitude of 42.7 m.

TABLE 6.— OUTPUT FROM PREFLIGHT SYNTHESIS

Table of commands

Waypoint	Time duration ΔT_i, sec	Turning[a] radius R_i, m	Acceleration $\dot{V}_i$, m/sec^2	Flight path angle γ_i, deg
1	75	0	0	0
	17.7	0	-.61	0
2	88	0	0	0
	17.7	0	-.61	0
3	33.1	-1371	0	0
4	33.1	-1371	0	-5.
5	25.7	0	0	-5.
	15.2	0	+.61	-5.
6				

[a]Above runway, runway at altitude of 42.7 m.

Min and Max time from waypoint to t final

Waypoint	Min time, sec	Max time, sec	Max time - min time, sec
1	305.5	335.1	29.6
2	212.8	231.7	18.9
3	107.1	111.3	4.2
4	74.0	78.2	4.2
5	40.9	45.1	4.2
6	0	0	0

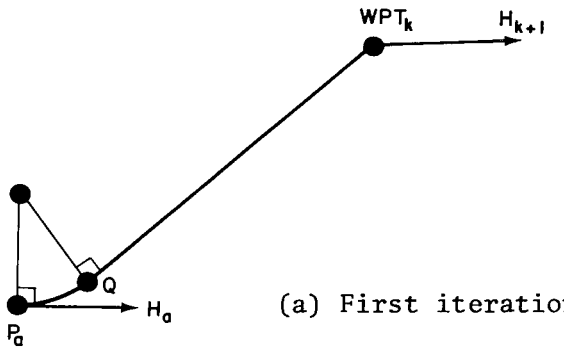

(a) First iteration.

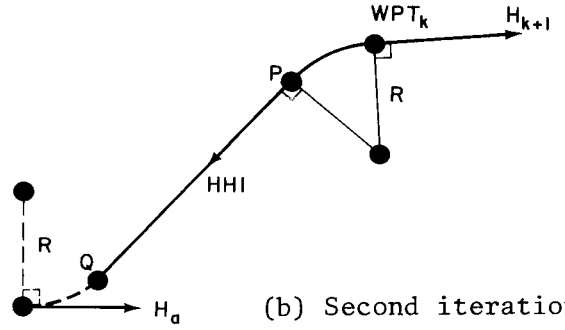

(b) Second iteration.

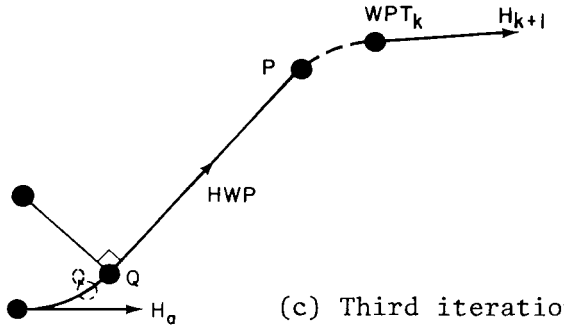

(c) Third iteration.

Figure 18.— Synthesizing capture trajectory.

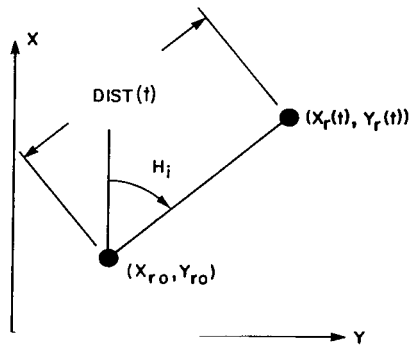

(a) For straight flight.

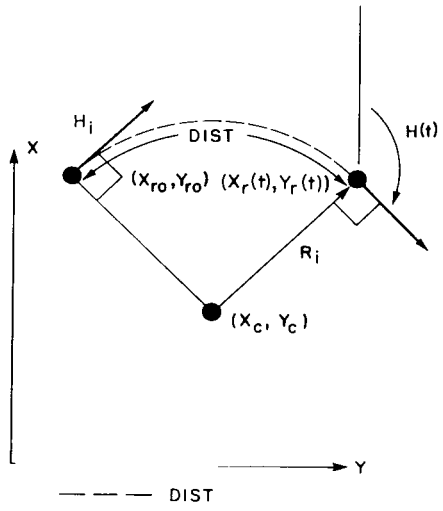

(b) Turn.

Figure 19.— Reference position computations.

are within 1° of each other, which means that P - Q is approximately tangent to both turns; if so, the capture flight path has been synthesized, and if not, iterate steps 2 through 4.

The synthesized horizontal flight path is displayed on the MFD (fig. 4(a)) in a dashed line. If a flight path does not exit, then a flashing NOCAP HOR message is on display. In synthesizing the vertical profile, if the computed flight-path angle is outside the range of permissible flight path angles, then a flashing NOCAP ALT message will be displayed. Similarly, in synthesizing the speed profile, if the straight flight distance is not sufficient to effect a speed change from the current aircraft speed to that specified at the waypoint, then a flashing NOCAP VEL message will be displayed. The overall

flight profile has now been synthesized and the control system will issue the proper command at the appropriate time.

Control system— The control system is described in detail in reference 2. Essentially, the control system generates the reference state as a function of time; incorporates the latest wind estimates from the navigation filter into the ground speed profile to generate the airspeed profile; generates the reference speed, bank angle, and flight-path angle commands; generates the feedbacks from along-track, cross-track, altitude, and heading errors; and generates the lead time for bank angle and flight-path angle commands.

The reference position is computed from an initial point (X_{ro}, Y_{ro}) for straight flight (see fig. 19(a)) and from a center of turn (X_c, Y_c) for turning flight (see fig. 19(b)) by equations (A15) and (A16):

$$\left.\begin{aligned} \begin{bmatrix} X_r(t) \\ Y_r(t) \end{bmatrix} &= \begin{bmatrix} X_{ro} \\ Y_{ro} \end{bmatrix} + DIST(t) \begin{bmatrix} \cos H_i \\ \sin H_i \end{bmatrix} \quad \text{for straight flight} \\ \begin{bmatrix} X_r(t) \\ Y_t(t) \end{bmatrix} &= \begin{bmatrix} X_c \\ Y_c \end{bmatrix} + R_i \begin{bmatrix} \sin H(t) \\ -\cos H(t) \end{bmatrix} \quad \text{for turn} \end{aligned}\right\} \tag{A15}$$

$$Z_r(t) = Z_{ro} - DIST(t) \tan \gamma_i \tag{A16}$$

where $DIST(t)$ is the ground distance the phantom aircraft has traversed since the beginning of the command segment. $DIST(t)$ is given by

$$DIST(t) = \int_{t_o}^{t} V_i(t)\, dt \tag{A17}$$

$$V_i(t) = V_{io} + \int_{t_o}^{t} \dot{V}_i\, dt \tag{A18}$$

where $V_i(t)$, V_{io} and $\dot{V}_i$ are the ground speed, the initial ground speed, and the commanded inertial acceleration for the phantom aircraft. The reference ground heading for a turn is computed by (fig. 19(b)):

$$H(t) = H_k + \frac{DIST(t)}{R_k} \tag{A19}$$

where H_k is the synthesized heading at waypoint k-1 and DIST the horizontal distance traversed by the phantom since the beginning of the turn.

The reference ground speed is next converted to reference TAS by the following relation,

$$\begin{bmatrix} V_x(t) \\ V_y(t) \\ V_z(t) \end{bmatrix} = \begin{bmatrix} \dot{X}_r(t) \\ \dot{Y}_r(t) \\ \dot{Z}_r(t) \end{bmatrix} - \begin{bmatrix} W_{xe}(t) \\ W_{ye}(t) \\ W_{ze}(t) \end{bmatrix} = V_i(t) \begin{bmatrix} \cos H(t) \\ \sin H(t) \\ \tan \gamma_i \end{bmatrix} - \begin{bmatrix} W_{xe}(t) \\ W_{ye}(t) \\ W_{ze}(t) \end{bmatrix} \tag{A20}$$

$$V_r(t) = (V_x^2 + V_y^2 + V_z^2)^{1/2} \tag{A21}$$

where (W_{xe}, W_{ye}, W_{ze}) are wind components from the navigation filter in runway coordinates.

For pilot convenience, indicated airspeed is used for specifying airspeed for the synthesizer and for flying the aircraft. However, ground speed must be used for computing the TOA and other time control elements. The synthesizer generates a ground speed profile based on the specified airspeed at waypoints and the pilot-entered wind estimate (EWMAG, EWANGL) shortly before the system is placed in track. Consequently, TOA and the time control elements were computed based on the best knowledge of the wind estimate before tracking.

In the track mode, the reference airspeed $V_r(t)$ for flying the aircraft is computed by taking the vector sum of the ground speed specified by the synthesizer and the wind estimate from the navigation filter ($W_{xe}(t)$, $W_{ye}(t)$, $W_{ze}(t)$) to take advantage of the latest available information. Therefore, it is necessary to go from VA_k, the specified airspeed, through $V_i(t)$ the ground speed, and back to airspeed $V_r(t)$. To reiterate, two wind estimates were incorporated in the speed computation, one based on the estimate before tracking and the other on the most current wind estimate. Ideally, these two estimates should be the same or very close to each other, and any difference between the two will be nulled out by the control law.

The reference heading $\psi_r(t)$ reference heading rate $\dot{\psi}_r(t)$, and reference bank angle $\phi_r(t)$ are computed by equations (A22), (A23), and (A24), respectively.

$$\psi_r(t) = \tan^{-} \frac{V_y}{V_x} \tag{A22}$$

$$\dot{\psi}_r(t) = \frac{\dot{V}_i}{V_i} \frac{(V_x\dot{Y}_r - V_y\dot{X}_r)}{(V_x^2 + V_y^2)^{1/2}} + \frac{V_i}{R} \frac{(V_x\dot{X}_r + V_y\dot{Y}_r)}{(V_x^2 + V_y^2)^{1/2}} \tag{A23}$$

$$\phi_r(t) = \tan^{-1}\left(\frac{\dot{\psi}_r V_r}{g}\right) \tag{A24}$$

The second term in equation (A23) is set equal to zero for straight flight. The aircraft coordinates are next expressed in a moving target reference with the position coordinates of the reference aircraft as the origin and the reference aircraft heading as the positive x axis (fig. 20). The transformation of the aircraft coordinate and heading is accomplished by the following relations,

$$\begin{bmatrix} x(t) \\ y(t) \\ z(t) \end{bmatrix} = \begin{bmatrix} \cos\ \psi_r(t) & \sin\ \psi_r(t) & 0 \\ -\sin\ \psi_r(t) & \cos\ \psi_r(t) & 0 \\ 0 & 0 & 1 \end{bmatrix} \begin{bmatrix} X_a(t) - X_r(t) \\ Y_a(t) - Y_r(t) \\ Z_a(t) - Z_r(t) \end{bmatrix} \tag{A25}$$

$$\psi(t) = \psi_a(t) - \psi_r(t) \tag{A26}$$

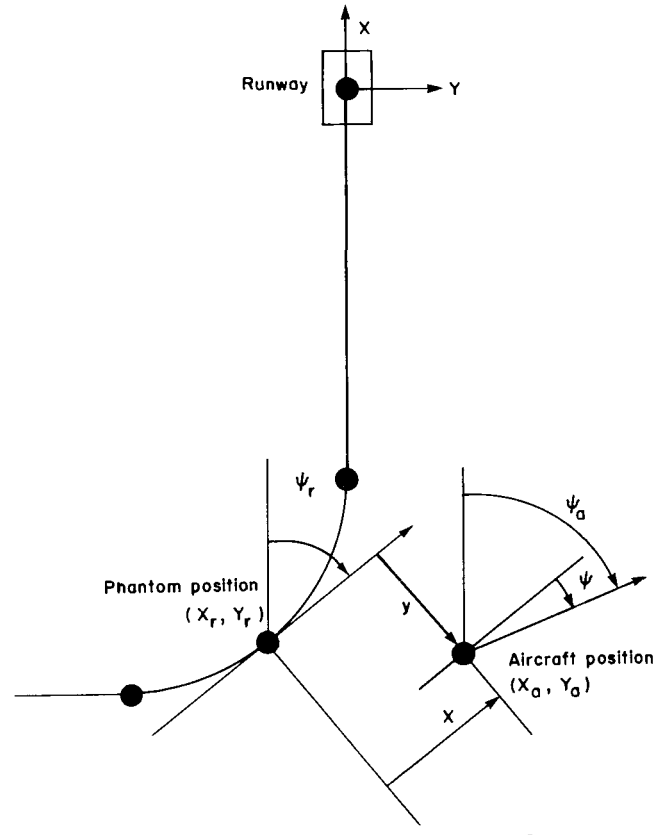

Figure 20.— Moving target reference.

The subscript a refers to aircraft quantities, and (x, y, z), ψ are errors in position coordinates and in heading. The velocity, bank angle, and flight-path angle commands for the fully automatic flight are generated by the following relations,

$$V_c(t) = V_r(t) - k_{vx}x(t) - k_{vy}\dot{\psi}_r y(t) + \Delta V(za) \tag{A27(a)}$$

$$\phi_c = \phi_r(t) - k_{\phi y}y(t) - k_{\phi\psi}V_r\psi(t) + k_{\phi x}\dot{\psi}_r x(t) \tag{A28(a)}$$

$$\gamma_c = \gamma_r - \frac{k_{\dot{z}z}z(t)}{V_{i/a}} \tag{A29(a)}$$

where k_{vx}, k_{vy}, $k_{\phi y}$, $k_{\phi\psi}$, $k_{\phi x}$, and $k_{\dot{z}z}$ are feedback gains, $V_{i/a}$ is the ground speed of the aircraft, and ΔV a factor for converting TAS to IAS. The corresponding flight director commands for the manual track mode are expressed by the relations,

$$V_c'(t) = V_c(t) - V_a(t) \qquad \text{(A27(b))}$$

$$\phi_c'(t) = \left[\phi_c(t) - \phi_a(t)\right] + K_\phi \dot{\phi}_a(t) \qquad \text{(A28(b))}$$

$$\theta_c'(t) = \left[\gamma_c(t) - \gamma_a(t)\right] + k_\gamma \dot{\gamma}_a(t) \qquad \text{(A29(b))}$$

where K_ϕ and K_γ are constants. The command $V_c'(t)$ is used to generate the display for the speed error indicator in the EADI, and $\phi_c'(t)$ and $\theta_c'(t)$, after passing through their respective position and rate limiters, are used to generate the display for the roll land pitch flight director bars in the EADI.

Lead bank angle and lead flight-path angle commands are introduced to reduce the cross-track and altitude errors that would result from the assumption of infinite bank rate and infinite flight-path angle rate in the synthesized trajectory. The lead time for bank angle and flight-path angle commands are given by the following,

$$\tau_\phi = \frac{\phi_{i+1} - \phi_i}{2\dot{\phi}_{max}} \qquad \text{(A30)}$$

$$\tau_\gamma = \frac{\gamma_i + \dot{\gamma}_{max}\ \gamma_{i+1}}{2\dot{\gamma}_{max}} \qquad \text{(A31)}$$

where $\phi_{i+1} - \phi_i$ is the difference between two consecutive reference bank angle commands, γ_i and γ_{i+1} the reference flight path angle commands and $\dot{\phi}_{max}$, $\dot{\gamma}_{max}$ are the maximum allowable bank rate and flight path angle rate, respectively.

Equation (A30) was derived (ref. 4) by matching the heading changes produced by a step in bank command with that produced by a ramp in bank command (fig. 21(a)). Similarly, equation (A31) was derived by matching the altitude change produced by a ramp in flight path angle command to that produced by a step in flight path angle command (fig. 21(b)).

The velocity command, expressed in indicated airspeed, consists of reference velocity, the velocity feedback (Eq. A27(a)) and a factor for converting TAS to IAS. The reference velocity is the vector sum of the ground speed specified by the command sequence and the wind estimate from navigation filter. The feedbacks for the velocity command include the along-track and cross-track errors.

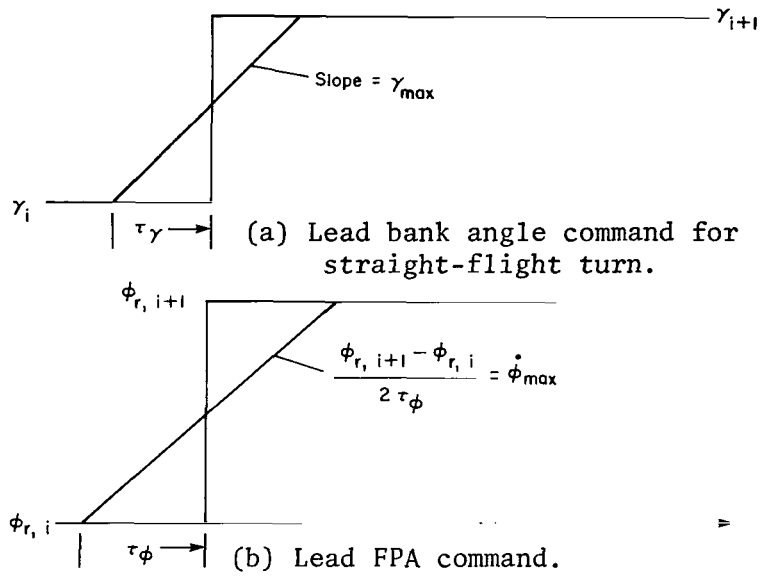

Figure 21.— Lead commands.

To prevent any unreasonable commands from being issued to the autothrottle or to the airspeed error bar, the velocity command is limited in three ways. First, it is limited by the upper and lower bounds of the control authority. The second limit is the minimum speed limit, which for the CV-340 was specified as 1.3 times the stall speed, which is turn is a function of the flap position. The third limit is the flap placard limit.

The two control bounds are expressed by U_b percent and L_b percent, specified by the pilot, as the maximum allowable deviation of the reference airspeed specified in the trajectory (U_b = 10 percent and L_b = -10 percent in the flight test). The reference speed is specified at waypoints and at any other point it is interpolated from speeds specified at adjacent waypoints. The TOA at the final waypoint is calculated for moving the phantom at a ground speed, which when vectorially summed with the wind speed entered from the keyboard will result in an airspeed that is exactly equal to the reference airspeed, provided that the keyboard entry equals the true wind. Therefore, the reference airspeed, $V_r(t)$, is not affected by wind estimates by either keyboard input or from the navigation filter.

At the final waypoint, it is important for the aircraft to fly at landing speed. Therefore, beginning at the next to the last waypoint, the control authority limits are linearly reduced from the specified percentages to zero at the last waypoint. In the automatic mode, the control system enables the autoflap logic if the current airspeed calls for flaps. In the manual tracking mode, the control system issues the flap deployment message on the MFD as required. Since the aircraft to be flown in the flight experiment has neither provision for deploying the flap automatically nor for monitoring the flap position, it is necessary that the flap-deployment message be based on current airspeed of the aircraft. The flap-deployment schedule is as follows: while flying the capture trajectory or if the airspeed exceeds 140 knots true

airspeed (KTAS), no flap; if the airspeed is between 130 and 140 KTAS, 17° flap; if the airspeed is between 120 to 130 KTAS, 28° flap; and finally, if the airspeed is below 120 KTAS and the final 5° glide slope is underway, 40° or full flap. The flap-deployment message is an implementation of this flap schedule.

The bank angle command consists of a reference bank angle and a feedback. During lead time, the reference bank angle is set to a precomputed value (eq. (A30)). During any other time, it is set equal to the value computed in equation (A24). The bank angle command is limited by ϕ_{max}, the maximum allowable bank angle, specified by the pilot for passenger comfort and safety consideration.

Similarly, the flight-path angle command consists of a reference flight-path angle and a feedback. The reference flight-path angle is set equal to precomputed values during lead time (Eq. (A31)) and to the value specified by the command sequence at any other time. The flight-path angle command is limited from above by γ_{max} and below by γ_{min}, the limits specified by the pilot for both passenger comfort and safety considerations.

The equations presented in this section were implemented in the trackmode computer program. Essentially, the program performs various computational tasks required for implementation of the control system discussed and distributes the allotted time for doing so. Distribution of computation time is accomplished by directing the flow of various logical paths shown in figure 23. The computational tasks are as follows:

1. Initialize the track mode.

2. Update the phantom state at waypoints, and generate the reference state, a set of commands for tracking, and the necessary messages for displays.

3. Compute the lead time and lead bank angle and lead flight-path angle commands.

4. Disconnect 4D and shift control to the conventional system at t final.

Executive Algorithm

The foregoing sections have described the elements of a 4D RNAV system, which computes the reference and capture flight paths from assigned waypoints and arrival times. However, an executive algorithm is required to make these elements function as a unit. This algorithm is a logic structure that calls basic support routines and 4D guidance and control routines for effecting the overall functioning of the 4D system. It evolved from extensive work, which included theoretical work, simulation experiments, and pilot opinion. As a result of this study, the following set of ground rules were incorporated into the algorithm to form the basic logical structure.

1. Fly conventional autopilot modes until the system is in track.

2. Select the best navigation aid available.

3. Synthesize a capture trajectory continuously in the predictive mode and permit specification of waypoint to be captured in the predictive mode only.

4. Display the reference trajectory as a solid line and the capture trajectory, if it exists, as a dotted line in the predictive mode and solid line in the track mode. If there is no feasible capture trajectory, state the reason as a flashing message on the MFD.

5. Permit wind entry for the purpose of synthesizing a new ground speed profile and recompute the time control elements in both the predictive and track mode. After the wind entry is processed while continuing in the track mode, the system automatically switches to the predictive mode to remind the pilot that TOA may have been altered and he must act accordingly, either to exercise the TDC command (after the system has been placed in track) to maintain the old TOA if possible or to place the system in track at the new TOA.

6. Permit time delay command (TDC) entry for fine TOA adjustment at the track mode only.

7. Use current aircraft state (position, heading, and speed) as the initial point of the reference aircraft to initialize tracking.

8. Update the reference aircraft state at waypoints, that is, set the phantom position, heading and ground speed equal to those specified/precomputed for the waypoint.

9. Incorporate lead time in both the bank angle and flight path angle commands to minimize the cross track and altitude error.

10. Display on the MFD excessive-error messages if the altitude, cross-track, or along-track errors exceed their respective prespecified values.

11. Limit the reference airspeed to within certain specified upper and lower percentages of the specified airspeed at waypoints, and certain interpolated values of specified airspeed between waypoints.

The executive algorithm incorporates the ground rules stated above, distributes the available time for execution of the appropriate algorithm, processes inputs from the pilot and the test conductor, directs the flow to the logical path specified by pilot inputs, and generates commands for the autopilot and the autothrottle in the automatic tracking mode.

Figure 22 is a functional block diagram of the Ames 4D executive algorithm, and its interrelation with inputs, displays and commands, and feedbacks. Pilot inputs to the 4D consist of four keyboard mnemonics and three switches on the MSP. The keyboard mnemonics are FOD for switching between 4D and

ordinary flight director modes, WPT for selection of waypoints, EWD for wind estimate input, and TDC for changing the TOA. The selection switches on the MSP are F/D for enabling the flight director, REF FP for switching between predictive mode and the flight director tracking, and FULL AUTO for switching between predictive mode and automatic tracking mode (for simulation only). The outputs consist of a set of commands V_c, ϕ_c, and γ_c for the autopilot and autothrottle in automatic tracking, and another set of commands V_c', ϕ_c', and γ_c' in flight director tracking. The displays include the reference flight path, the capture trajectory, pertinent messages for the MFD and the flight director commands and path position errors in the EADI. The pilot inputs and the displays are discussed in detail in the section entitled "Pilot's Operating Procedure."

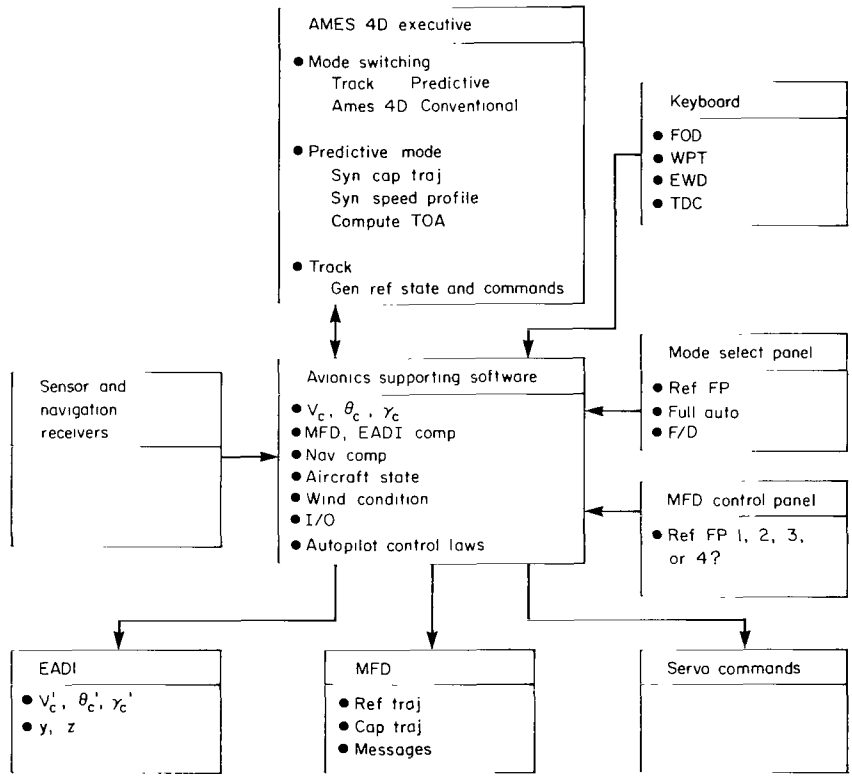

Figure 22.— Interfacing of Ames 4D executive algorithm.

Figure 23 is a macro flowchart of the executive algorithm. In the mode-selection stage, the proper flag is set up to execute the desired mode, Ames 4D or conventional A/P or F/D modes. If the system is in Ames 4D, a

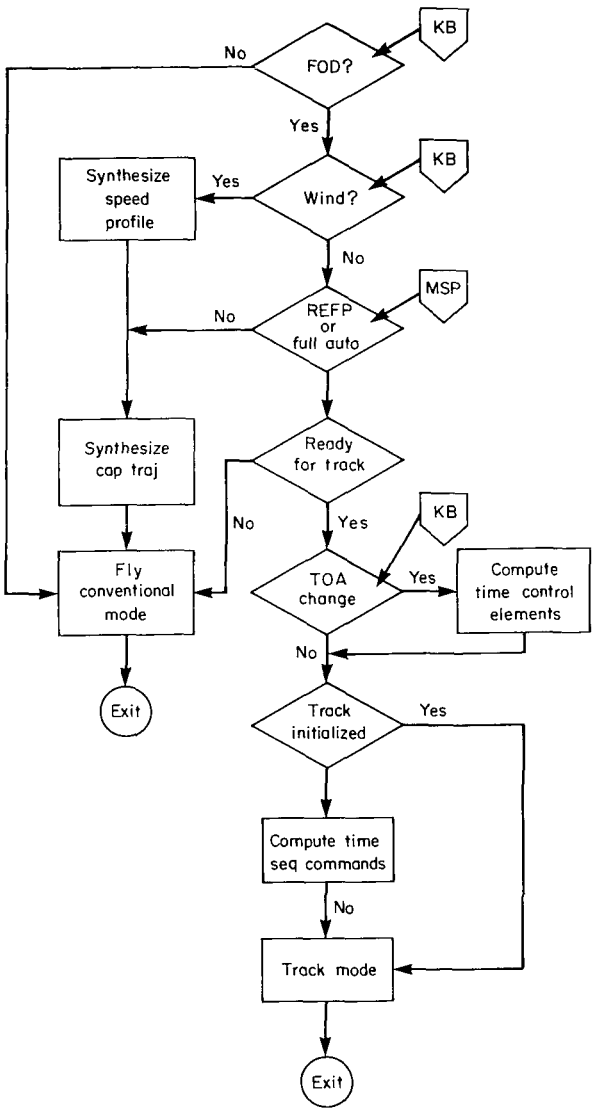

Figure 23.— Ames 4D executive algorithm — micro flow chart.

check is made if it is in the predictive or track mode. If in track, a further check is made if flight director or automatic mode is selected. Next, the executive program detects any new wind estimate input and processes it by directing the flow to the ground speed profile synthesis, time control elements, and command table computation. Then it detects if the system is in track and, if not, directs the flow to the capture trajectory synthesis. If the system is in track, it detects any TOA changes (via TDC input) and directs the flow to recompute time control elements and continues tracking. Otherwise, it proceeds to ascertain if the command sequence has been generated and, if not, directs the flow to command sequence generation. If the sequence has already been generated, the algorithm directs the flow to the track mode.

One of the critical functions of the executive algorithm is timing. The Ames 4D system is limited to 5 msec of execution for every sampling period of 50 msec. Many of its algorithms cannot be executed in the alloted 5 msec in a single pass. Therefore, some of the computation is accomplished in several passes and one of the functions of the executive is to distribute the available time to various parts of different algorithms so that the whole program is executed most efficiently. The wind input is processed in three passes, the capture trajectory is synthesized in no more than six passes and the TOA change input is processed along with tracking computations. In the track mode, odd passes are allotted to control system computation and even passes for precomputation of lead time, lead bank angle, and lead flight-path angle commands.

REFERENCES

1. Erzberger, H.; and Lee, H. Q.: Terminal Area Guidance Algorithms for Automated Air Traffic Control. NASA TN D-6773, 1972.

2. Lee, H. Q.; McLean, J.; and Erzberger, H.: Guidance and Control Technique for Automated Air Traffic Control. J. Aircraft, vol. 9, no. 7, July 1972, pp. 490-496.

3. Erzberger, H.; and Pecsvaradi, T.: 4D Guidance System Design with Application to STOL Air Traffic Control. 1972 JACC of the American Automatic Control Council, held on Aug. 16-18, 1972, Stanford, Ca., pp. 445-454.

4. Pecsvaradi, Thomas: Algorithms for 4D Guidance in an ATC Environment. NASA TN D-7829.

5. Civil Aviation Research and Development Policy Study - Report. NASA SP-265, 1971. (Also available as DOT TST-10-4.)

6. Civil Aviation Research and Development Policy Study - Supporting Papers. NASA SP-266, 1971. (Also available as DOT TST-10-5.)

7. Hansen, Q. M.; Young, L. S.; Rouse, W. E.; and Osder, S. S.: Development of STOLAND, a Versatile Navigation Guidance and Control System. AIAA 4th Aircraft Design Flight Test and Operations Meeting, Paper No. 72-789, Los Angeles, Aug. 7-9, 1973.

8. Neuman, F.; and Warner, David N., Jr.: A STOL Terminal Area Navigation System. NASA TM X-62,348, May 1974.

9. Smith, D. W.; Neuman, F.; Watson, D. M.; and Hardy, G. H.: A Flight Investigation of Terminal Area Navigation and Guidance Concept for STOL Aircraft. NASA Advanced Control Technology Symposium, Los Angeles, July 9-11, 1974.

10. Pecsvaradi, Thomas: Optimal Horizontal Guidance Law for Aircraft in the Terminal Area. IEEE Trans. Automatic Control, vol. AC-17, no. 6, Dec. 1972.

"The aeronautical and space activities of the United States shall be conducted so as to contribute . . . to the expansion of human knowledge of phenomena in the atmosphere and space. The Administration shall provide for the widest practicable and appropriate dissemination of information concerning its activities and the results thereof."

—NATIONAL AERONAUTICS AND SPACE ACT OF 1958

NASA SCIENTIFIC AND TECHNICAL PUBLICATIONS

TECHNICAL REPORTS: Scientific and technical information considered important, complete, and a lasting contribution to existing knowledge.

TECHNICAL NOTES: Information less broad in scope but nevertheless of importance as a contribution to existing knowledge.

TECHNICAL MEMORANDUMS: Information receiving limited distribution because of preliminary data, security classification, or other reasons. Also includes conference proceedings with either limited or unlimited distribution.

CONTRACTOR REPORTS: Scientific and technical information generated under a NASA contract or grant and considered an important contribution to existing knowledge.

TECHNICAL TRANSLATIONS: Information published in a foreign language considered to merit NASA distribution in English.

SPECIAL PUBLICATIONS: Information derived from or of value to NASA activities. Publications include final reports of major projects, monographs, data compilations, handbooks, sourcebooks, and special bibliographies.

TECHNOLOGY UTILIZATION PUBLICATIONS: Information on technology used by NASA that may be of particular interest in commercial and other non-aerospace applications. Publications include Tech Briefs, Technology Utilization Reports and Technology Surveys.

Details on the availability of these publications may be obtained from:

SCIENTIFIC AND TECHNICAL INFORMATION OFFICE

NATIONAL AERONAUTICS AND SPACE ADMINISTRATION

Washington, D.C. 20546